

Modeling the carbon fluxes of the northwest European continental shelf: Validation and budgets

S. L. Wakelin,¹ J. T. Holt,¹ J. C. Blackford,² J. I. Allen,² M. Butenschön,² and Y. Artioli²

Received 23 June 2011; revised 27 January 2012; accepted 28 March 2012; published 12 May 2012.

[1] Carbon budgets are simulated for the northwest European continental shelf and adjacent regions of the northeast Atlantic. Both physical and biological processes are evaluated, including exchanges between the water column and the atmosphere and sea bed.

We use a multi-year simulation of a coupled 3D hydrodynamics-ecosystem model (POLCOMS-ERSEM) driven by realistic atmospheric data, ocean boundary conditions and freshwater inputs for 1989 to 2004. The northeast Atlantic (20°W to 13°E, 40°N to 65°N), including the European shelf, is found to be a net sink for atmospheric CO₂. Biological processes exert a stronger control over pCO₂ than temperature, and hence have a stronger effect on the air-sea CO₂ exchange. For the European shelf, carbon sources of rivers and the uptake of atmospheric CO₂ are balanced by horizontal transport off shelf and there is little carbon burial. There is net transport of carbon onto the shelf in the top 180 m of the water column and off the shelf below that depth, with a net carbon loss of $\sim 6 \pm 1 \times 10^{12}$ mol C yr⁻¹. Up to 50% of the carbon exported from the shelf is transported below the permanent pycnocline and so is isolated from release into the atmosphere on centennial timescales.

Citation: Wakelin, S. L., J. T. Holt, J. C. Blackford, J. I. Allen, M. Butenschön, and Y. Artioli (2012), Modeling the carbon fluxes of the northwest European continental shelf: Validation and budgets, *J. Geophys. Res.*, 117, C05020, doi:10.1029/2011JC007402.

1. Introduction

[2] The oceanic carbon sink is a vital component of the Earth System removing $\sim 26\%$ of the anthropogenic atmospheric CO₂ inputs [Le Quéré *et al.*, 2009], and hence substantially mitigating the consequences for global climate change. One of the greatest sources of uncertainty in the oceanic carbon budget is the contribution of shelf and coastal seas [e.g., Borges, 2005]. This component is poorly represented in both global models and global climatologies. Hence, fine resolution regional models provide an important tool for assessing the processes involved in this flux and potentially reducing the uncertainties.

[3] The North Atlantic has been identified as an important sink for CO₂, accounting for 23% of the anthropogenic carbon stored by the oceans while covering only 15% of the global ocean surface [Sabine *et al.*, 2004]. Whilst much of the uptake of CO₂ takes place in the open ocean [Schuster and Watson, 2007; Takahashi *et al.*, 2002], the northwest European continental shelf also plays a significant role through the mechanism of the shelf sea carbon pump. Originally proposed by Tsunogai *et al.* [1999] in the context of the East China Sea, this process has also been observed in the North Sea [Thomas *et al.*, 2004; Bozec *et al.*, 2005]. The basis of

the carbon pump in seasonally stratified shelf seas is as follows. Phytoplankton production in the spring bloom and mid water chlorophyll maximum exports particulate organic carbon (POC) below the summer pycnocline where it remains isolated from atmospheric exchange as long as the water column is stratified, even if the POC is re-mineralized to dissolved inorganic carbon (DIC). If this below-pycnocline water (BPW) is transported off the shelf to the deep ocean, then this may represent a substantial sequestration of atmospheric carbon. Frankignoulle and Borges [2001] estimate that the northwest European continental shelf takes up from the atmosphere an additional $\sim 45\%$ of CO₂ compared to the fluxes proposed by Takahashi *et al.* [1995] for the open North Atlantic Ocean.

[4] In the absence of substantial long-term burial of POC in sediments (discussed below), the efficiency of the shelf sea carbon pump is to a large extent dictated by the transport of BPW off the shelf and below a permanent pycnocline before the winter breakdown of stratification. On the northwest European shelf, at first glance, this looks unpromising since the dominant transport pathway off-shelf is in a surface current (the Norwegian coastal current) suggesting that carbon sequestered on the shelf is returned to the atmosphere in the Norwegian Sea, although the temperature gradient would tend to inhibit this as the water cools on its northwards journey and the partial pressure of CO₂ in the water is reduced. In addition to the large scale circulation pattern, at the shelf edge the bottom Ekman layer, a frictionally driven down-slope flow below the slope current [Huthnance, 1995; Souza *et al.*, 2001], provides an alternative mechanism for transporting BPW off-shelf. Holt *et al.* [2009] used a 45-year

¹National Oceanography Centre, Liverpool, UK.

²Plymouth Marine Laboratory, Plymouth, UK.

Corresponding author: S. L. Wakelin, National Oceanography Centre, 6 Brownlow St., Liverpool L3 5DA, UK. (slwa@noc.ac.uk)

Copyright 2012 by the American Geophysical Union.
0148-0227/12/2011JC007402

hydrodynamic simulation of the northwest European continental shelf to estimate carbon export from the shelf based on the transport of a passive tracer, integrated over time periods and depths to capture the effects of the spring phytoplankton bloom and sinking of detritus. They show that the large scale circulation and frictional processes potentially transport carbon off the shelf sufficiently quickly to remove $\sim 40\%$ of the carbon sequestered by one growing season before the onset of the next. This transport is highly heterogeneous, with some regions exporting little carbon from the shelf. Of the exported carbon, 52% is transported below the permanent pycnocline [Holt *et al.*, 2009], hence the shelf sea and open ocean carbon cycles are intrinsically coupled. Using a one-box carbon budget model for the North Sea based on modeled and observed estimates of the water budget and carbon parameters, Thomas *et al.* [2005a] found that the region is an efficient carbon pump with more than 90% of the carbon taken up from the atmosphere exported to the North Atlantic, although the processes transporting water to the deep ocean were not considered.

[5] There have been several observational campaigns examining the carbon cycle in the North Atlantic on all scales from estuaries [e.g., Frankignoulle *et al.*, 1998; Borges *et al.*, 2006] to the whole North Atlantic [e.g., Schuster and Watson, 2007; Schuster *et al.*, 2009]. On a regional scale, Thomas *et al.* [2004], Bozec *et al.* [2005], and Schiettecatte *et al.* [2007] used observations from the North Sea to show that the region is a sink for atmospheric CO_2 . Frankignoulle and Borges [2001] present data for the southern North Sea, the Bay of Biscay and the Celtic Sea and demonstrate that, except for during some winter sampling, the flux of CO_2 is always from atmosphere to sea, while Borges and Frankignoulle [2003] conclude that the English Channel is not a major sink of CO_2 . Borges and Frankignoulle [2002] use observations off the Spanish Galician coast under both upwelling and downwelling conditions to conclude that this region is also a CO_2 sink. There is, however, evidence that most near-shore coastal areas and inner estuaries in Europe are over-saturated with respect to CO_2 and act as sources to the atmosphere [Frankignoulle *et al.*, 1998; Borges *et al.*, 2006; Chen and Borges, 2009]. What is clear is that there is significant spatial and temporal heterogeneity in the system, driven by strong biological and physical processes. This may bias regional budgets derived from necessarily limited sampling programmes and hence models, guided by observations, are an important alternative tool.

[6] Several modeling studies have been used to investigate the carbon cycle on global and oceanic scales. Yool and Fasham [2001] use an open ocean general circulation model with a parameterization of the continental shelf pump to investigate the contribution of continental shelves to the global ocean carbon cycle and conclude that the continental shelves are potentially responsible for a net oceanic CO_2 uptake of $\sim 0.6 \text{ Gt C yr}^{-1}$. Smith and Marotzke [2008] investigate the factors influencing the uptake of anthropogenic carbon under different CO_2 forcing scenarios and find that the North Atlantic is a sink for atmospheric CO_2 and that the physical aspects of climate change are expected to strengthen the effects of increased CO_2 storage in reducing the future uptake of anthropogenic CO_2 .

[7] Models specifically designed for use in coastal/shelf seas have the potential to improve over these open-ocean

model simulations through their enhanced resolution and improved process representation (e.g., through the inclusion of tidal mixing, improved topographic representation by terrain-following vertical coordinates and more realistic terrestrial boundary conditions). Modeling studies of the northwest North Atlantic Ocean [Fennel and Wilkin, 2009; Fennel, 2010] have been used to generate carbon budgets for the continental margin of the eastern coast of North America and show this region to be a net sink for atmospheric CO_2 , but with no systematic difference between the CO_2 uptake on the shelf and in the adjacent deep ocean. Modeling studies on the northwest European continental shelf have focused on the North Sea. Lenhart *et al.* [2004] use the ERSEM model in a box configuration to construct a carbon budget under conditions of high and low North Atlantic Oscillation (NAO) index and find that the net transfer of material from organic to inorganic in the North Sea is strongest under conditions of high NAO index. Gypens *et al.* [2004] use the MIRO-CO2 model to study the relative importance of temperature, biological processes and river inflows on the CO_2 air-sea exchange and show that the Belgium coastal zone (BCZ) is a small annual sink for CO_2 and is strongly affected by biological processes, while the western English Channel is in near equilibrium and is more strongly influenced by temperature. Using a 0D implementation of MIRO-CO2 for the period 1951 to 1998, Gypens *et al.* [2009] suggest that, at different times, the BCZ has been a net source and a net sink of atmospheric CO_2 and show that inorganic river nutrient loads exert a strong control on the air-sea flux of CO_2 here. Prowe *et al.* [2009] use the ECOHAM model to study the effects of overflow production on CO_2 drawdown in two distinct regions in the North Sea, and find high net CO_2 uptake in the seasonally stratified northern region and a weak net source in the permanently mixed southern region. Kühn *et al.* [2010] also use ECOHAM to generate a carbon budget for the North Sea, distinguishing between physically- and biologically-driven carbon fluxes for 1995–1996, under conditions of contrasting high and low NAO index and also conclude that the southern North Sea is a net source of atmospheric CO_2 while the northern North Sea is a net sink, both fluxes being stronger under conditions of high NAO index.

[8] The purpose of this paper is to estimate the carbon budget of the whole northwest European continental shelf and hence test the hypothesis that the shelf pump is a significant transport mechanism by which biological carbon sequestered on the shelf is exported to the deep waters of the North Atlantic. To address this we consider a 16-year simulation (1989–2004) of the NW European shelf using the Proudman Oceanographic Laboratory Coastal Ocean Modelling System (POLCOMS) [Holt and James, 2001] coupled to the European Regional Seas Ecosystem Model (ERSEM) [Blackford *et al.*, 2004]. The simulation extends over the whole shelf and into the deep water of the North Atlantic Ocean and covers a more extensive region than earlier carbon budget studies using ecosystem models in this region. Hence it can be used to investigate the details of exchange between the shelf and the North Atlantic, explore contrasting shelf sea regions and study inter-annual variability. The modeling approach allows the construction of a detailed budget and the investigation of fluxes at high spatial resolution using complete annual cycles.

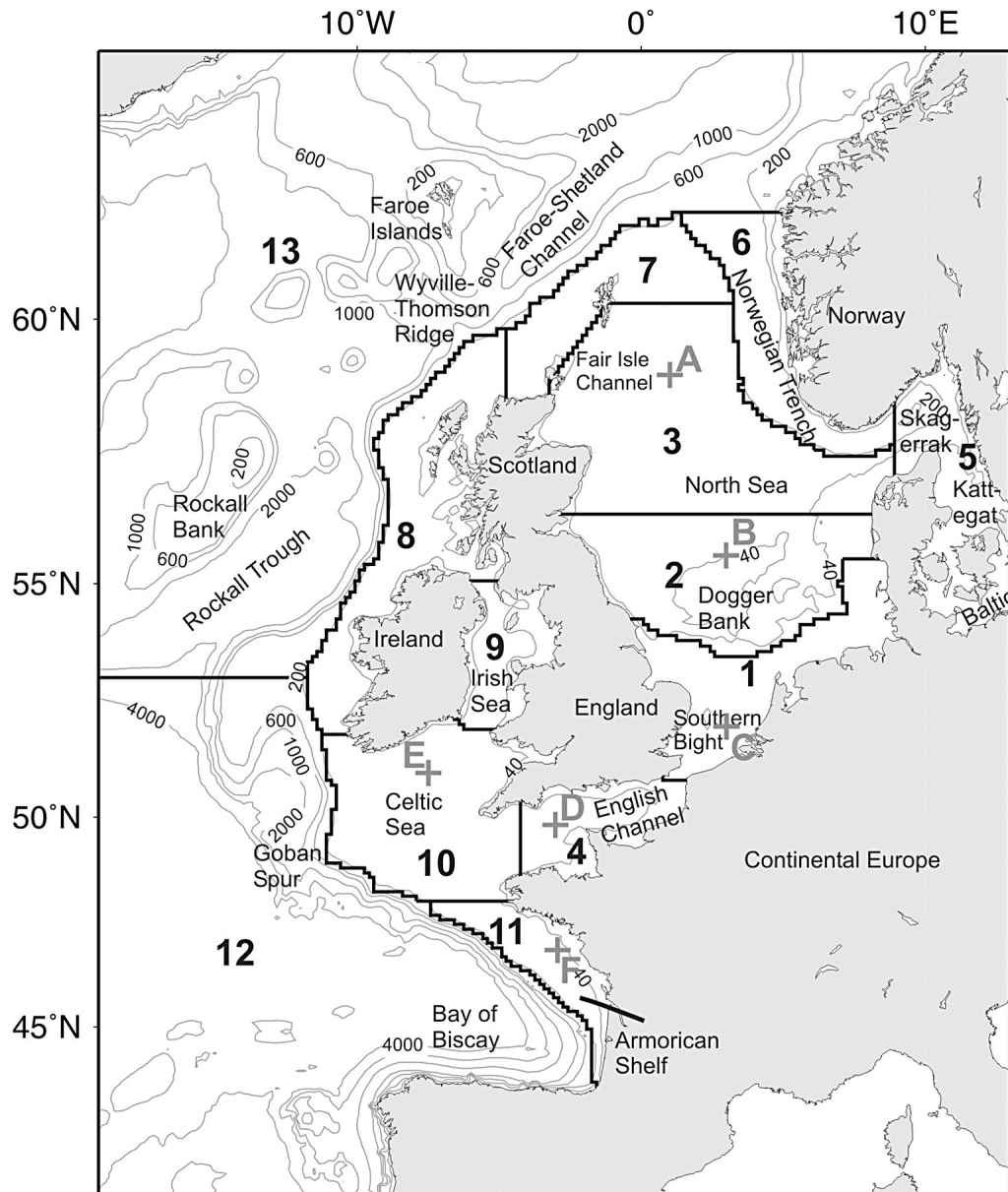


Figure 1. The model domain and bathymetry. Also shown are the 13 regions used for flux and budget calculations (labeled 1 to 13) and the 6 points (crosses) used for time series (labeled A to F).

[9] The simulation provides important insight into the nature of the carbon budget on the northwest European continental shelf and a baseline simulation against which future developments can be judged. It is, however, subject to the considerable uncertainty inherent in coupled hydrodynamics-ecosystem models as a consequence of the approximations involved. Hence, we use a wide range of biogeochemical observations to validate the simulation. The uncertainty associated with the POLCOMS-ERSEM coupled model has been extensively investigated particularly with the North Sea Project data [Allen *et al.*, 2007; Holt *et al.*, 2005] and Continuous Plankton Recorder data [Lewis *et al.*, 2006].

[10] Model experiments and analysis are described in the next section, followed by the model validation and error analysis in section 3. Carbon budgets are described in section 4,

while in section 5 the relative effects of temperature and biological controls on $p\text{CO}_2$ are discussed.

2. Model Setup

[11] We use the coupled hydrodynamic-ecosystem model POLCOMS-ERSEM on the Atlantic Margin domain extending from 20°W to 13°E and 40°N to 65°N (Figure 1), with resolution 1/9° latitude by 1/6° longitude (~ 12 km) and 42 s -coordinate [Song and Haidvogel, 1994] levels in the vertical.

[12] The implementation of the hydrodynamic model (POLCOMS) is that described by Wakelin *et al.* [2009], apart from an increase in the number of vertical levels to 42. The model is initialized at rest with temperature and salinity fields for 1st January 1984 taken from a 45-year integration (starting in 1960) of the hydrodynamics-only model [Holt *et al.*,

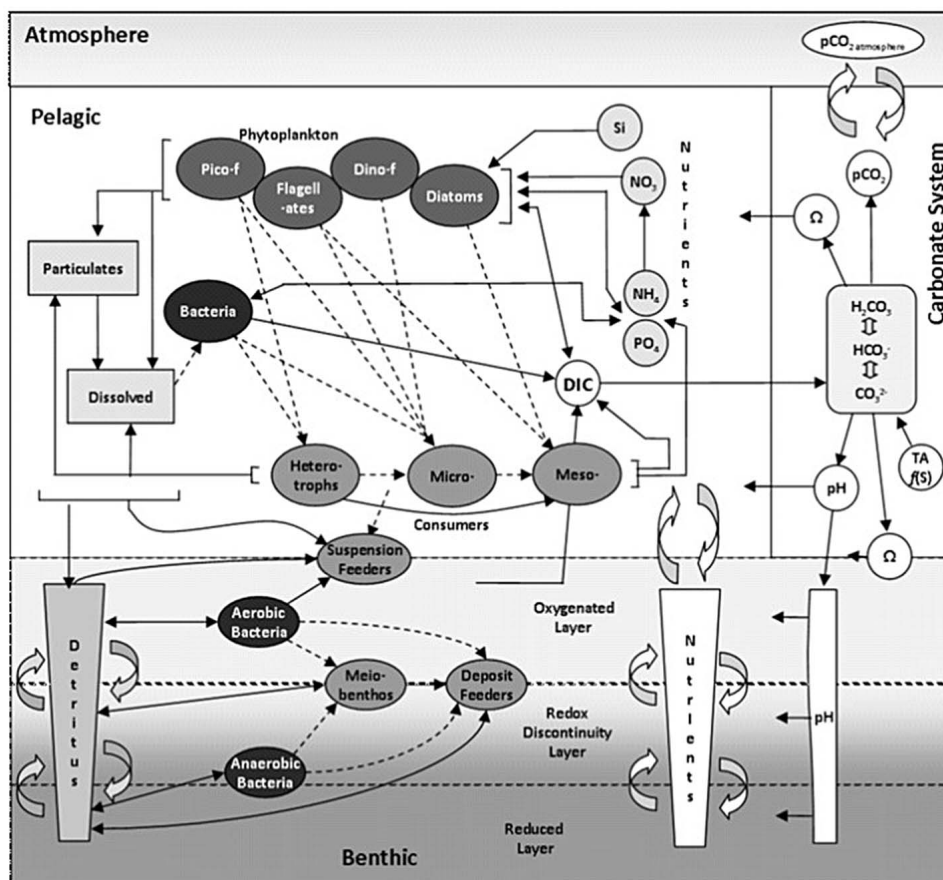


Figure 2. A schematic of the pelagic and benthic sub-models of ERSEM.

2009]. Surface forcing is provided by European Centre for Medium-Range Weather Forecasts (ECMWF) 40 year Re-Analysis (ERA40) data until September 2002 and thereafter by ECMWF operational analyses. Surface fluxes are derived from COARE3 bulk formulae [Fairall *et al.*, 2003]. Time-varying open boundary conditions are taken from a 1° global implementation of the Nucleus for European Modelling of the Ocean (5-day means available for 1960–2004 [Smith and Haines, 2009]) and 15 tidal constituents from a northeast Atlantic tidal model [Flather, 1981].

[13] The application of ERSEM is essentially that described by Blackford *et al.* [2004]. The structure of the model ecosystem is shown in Figure 2. An important aspect of the ERSEM model is that the carbon and nutrient cycles are decoupled through variable cell quotas. This allows the effects of recycled production on carbon drawdown to be accurately modeled. The main difference from the Blackford *et al.* [2004] model is the addition of a carbon chemistry module. The carbonate chemistry system is described by Blackford and Gilbert [2007] and uses the Mehrbach *et al.* [1973] constants as refitted by Dickson and Millero [1987], which are recognized as standard by the Ocean Carbon-Cycle Model Intercomparison Project (OCMIP) protocol. The carbon chemistry module uses an iterative method based on HALTAFALL [Ingri *et al.*, 1967], which is parameterized by total inorganic carbon (an ERSEM variable) and total alkalinity. Total alkalinity is parameterized as a function of salinity: $TA = (66.96S - 36.803)$, where the salinity $S \geq 34.65$

[Bellerby *et al.*, 2005] and $TA = (3887.0 - 46.25S)$, in coastal regions where $S < 34.65$ [Blackford and Gilbert, 2007]. The resulting partial pressure of CO_2 , together with the concentration of atmospheric CO_2 and the transfer velocity due to Nightingale *et al.* [2000], is used to calculate the air-sea CO_2 exchange. Levels of atmospheric CO_2 are represented by a time series of daily values calculated using data from the Azores, Mt Cimone in Italy and Mace Head in Ireland (J. Remedios and R. Leigh, personal communication, 2007) and include both an annual cycle and the increasing trend.

[14] The parameterization of alkalinity based on salinity [Blackford and Gilbert, 2007] provides a first order estimation that captures both the oceanic and coastal influences on alkalinity. It is however clear from several recent studies [e.g., Thomas *et al.*, 2009; Suykens *et al.*, 2010; Kim and Lee, 2009; Raymond and Cole, 2003; Fennel *et al.*, 2008] that alkalinity in regions of high biological dynamics and coastal influences demonstrates dynamics on a range of scales which are capable of influencing carbonate chemistry, pCO_2 and the resulting air-sea flux. Thomas *et al.* [2009] suggest that air-sea fluxes could increase by around 15% due to denitrification and Suykens *et al.* [2010] suggest that calcification could decrease air sea fluxes by about the same order of magnitude. However these dynamics are likely to be restricted spatially or temporally and would be far less significant over regionally integrated scales. There is clearly a need for comprehensive data to evaluate alkalinity seasonally, spatially and inter-annually, for mechanistic parameterizations of alkalinity

generation and for comprehensive riverine data to improve the accuracy of alkalinity simulation.

[15] The ecosystem model uses homogeneous initial conditions [Holt *et al.*, 2005] whilst boundary conditions for silicate, nitrate and phosphate are derived from monthly mean fields from the World Ocean Atlas [Garcia *et al.*, 2006]. A consequence of using climatological nutrient boundary conditions is that inter-annual variability of the ecosystem processes will depend only on the variability of the hydrodynamics and the atmospheric and riverine forcings in the region; far-field effects from the wider North Atlantic will not be included. This might be expected to affect on-shelf production on timescales of 5–10 years [Holt *et al.*, 2012].

[16] The calculation of non-biotic light attenuation differs from previous implementations of this model. Rather than using a sediment particulate matter (SPM) transport model, we use absorption estimates from SeaWiFS, specifically a mean annual cycle of 8-day composite absorption of SPM and colored dissolved organic matter (CDOM), based on 1998–2007 SeaWiFS data on a ~ 9 km grid. These are derived from the bio-optical model of Smyth *et al.* [2006]. A new model variable (a_{det}) is introduced for the inherent optical properties (IOP), representing CDOM and SPM concentrations. a_{det} is initialized to the observed winter mean values and transported along with the other state variables. When an observation is available, a_{det} is relaxed to this value throughout the water column with a time scale of 7 days. This simple, interpolation-based assimilation scheme removes some of the uncertainties associated with modeling SPM and CDOM directly (particularly sources, sinks and chemistry) and overcomes issues of model drift, caused by inaccuracies in material fluxes, that are apparent in multi-annual simulations. This method gives a seasonal cycle of the attenuation based on observations, but the high frequency variability is lacking; the effects of removing this variability are the subject of future investigation. The total diffuse attenuation, K_d , is defined as

$$K_d = a_{\text{det}} + a_{\text{phyt}} + a_w, \quad (1)$$

where the absorption components are: a_{det} , SPM and CDOM absorption constrained to SeaWiFS observations; a_{phyt} , phytoplankton absorption, linearly related to the four ERSEM phytoplankton carbon biomass variables; and a_w , a constant pure water component [Pope and Fry, 1997]. More sophisticated approaches, where K_d is a function of backscatter and sun angle, are also under investigation.

[17] In order to accurately model the transport of POC (especially detrital material) across the shelf a resuspension flux has been included in the ERSEM model. It reproduces the one used in the POLCOMS SPM transport model [Holt and James, 1999]. Settling occurs when the bed stress, τ , is less than a critical value ($\tau_{\text{dep}} = 0.01^2 \text{ m}^2 \text{ s}^{-2}$), and erosion occurs when a critical stress ($\tau_{\text{ero}} = 0.02^2 \text{ m}^2 \text{ s}^{-2}$) is exceeded. So the flux of POC from the benthic model to the pelagic model is

$$\begin{aligned} F &= w_s C (1 - \tau/\tau_{\text{dep}}) & \tau < \tau_{\text{dep}} \\ F &= M (\tau/\tau_{\text{ero}} - 1) & \tau > \tau_{\text{ero}} \end{aligned} \quad (2)$$

where w_s is the settling velocity (-0.5 , -2 and -10 m day^{-1} for small, medium and large particles, respectively), C is the concentration of each component and the erosion constant $M = 100 \times \tau_{\text{ero}} (\tau/\tau_{\text{ero}} - 1) F$, which is the total material eroded [Holt and James, 1999], modulated by F , the fraction of the bed sediment available for resuspension.

[18] Daily discharge data for 279 rivers are taken from the Global River Discharge Data Base (<http://grdc.bafg.de/>) and from data prepared by the Centre for Ecology and Hydrology (CEH) as described by Young and Holt [2007]. Mean annual cycles of riverine nutrient concentrations are obtained from the UK Environment Agency for 36 major UK and continental rivers. For rivers not included in the database, a mean annual cycle of the 36 rivers is used.

[19] Riverine sources of DIC are accounted for using a single mean annual cycle of DIC concentration for all rivers, in conjunction with the river discharge rates. The DIC time series has a mean value of $2680 \text{ mmol C m}^{-3}$ [Pätsch and Lenhart, 2004], with an annual cycle constructed to vary between a maximum value of $2766 \text{ mmol C m}^{-3}$ at the beginning and end of the year and a minimum of $2478 \text{ mmol C m}^{-3}$ at the end of May. Hence riverine sources of DIC include variability in river flows, but have a fixed annual cycle of DIC concentration. The mean value of $2680 \text{ mmol C m}^{-3}$ used here for DIC is higher than the $2590 \text{ mmol C m}^{-3}$ used by Thomas *et al.* [2005a]. Riverine concentrations of dissolved organic carbon (DOC) and POC are set to values in the river inflow grid box. This corresponds to an average DOC + POC concentration of 97 mmol C m^{-3} for 1989–2004, with values for individual rivers ranging from 21 to $191 \text{ mmol C m}^{-3}$. For comparison, Thomas *et al.* [2005a] use concentrations of DOC + POC of $\sim 293 \text{ mmol C m}^{-3}$ for rivers flowing into the North Sea.

[20] A mean annual inflow cycle is used for the Baltic, with a constant concentration of $2119 \text{ mmol C m}^{-3}$ [Thomas *et al.*, 2003] for DIC and a mean value of DOC + POC of $107 \text{ mmol C m}^{-3}$, taken from the values in the inflow boxes, in the same way as for the river inflows (compared to the value of 78 mmol C m^{-3} used by Thomas *et al.* [2005a]). Flow from the North Sea to the Baltic is not considered as only a depth integrated boundary condition is considered here.

[21] The results presented here are from a 21-year (1984 to 2004) run of POLCOMS-ERSEM; the first five years are treated as spin-up and 16 years are included in the analysis. Five years is ample spin-up time for the physics and pelagic biology on the Atlantic Margin domain, where, for example, the effect of the initial condition on the temperature field is small after ~ 2 years [Wakelin *et al.*, 2009]. For the ERSEM model, the flux of DIC from the benthos into the water column in the open ocean (depths $> 200 \text{ m}$) is the slowest term in the carbon budget to reach an approximately steady state. However, after five years, the trend in the DIC flux is greatly reduced (see below).

3. Model Validation

[22] Observations taken from the World Ocean Database 2005 (http://www.nodc.noaa.gov/OC5/WOD05/pr_wod05.html) are used for model validation. For the period of the model run, the database contains more than 400,000 measurements

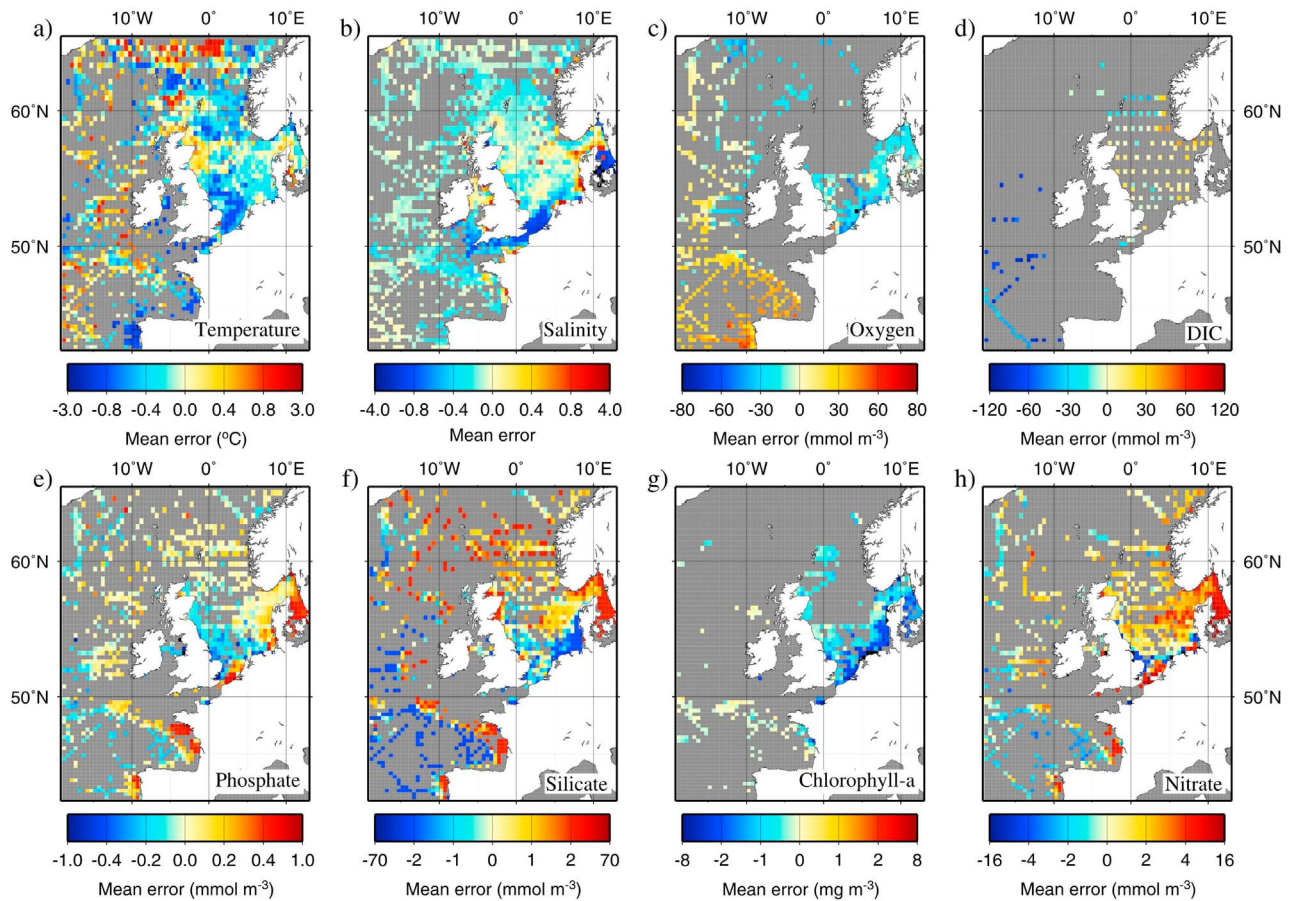


Figure 3. Mean errors (model – observation) for (a) temperature, (b) salinity, (c) oxygen, (d) dissolved inorganic carbon (DIC), (e) phosphate, (f) silicate, (g) chlorophyll-a, and (h) nitrate. Values are averaged onto $1/2$ by $1/3$ degree squares.

of temperature, a similar number of salinity measurements, over 120,000 measurements for each of the biogeochemical variables oxygen, silicate, phosphate, nitrate and chlorophyll-a and ~ 7000 DIC observations. A further ~ 2000 DIC observations from RV Pelagia cruises in the North Sea during 2001–2002 are also used [Thomas, 2002]. Modeled temperature and salinity, saved as 25-hour (approximately a tidal lunar day) means, are extracted co-located in space and time with each observation and the mean error (model – observed) is calculated by averaging over $1/2^\circ$ longitude by $1/3^\circ$ latitude grid squares (Figure 3). The normalized root-mean-square (RMS) error (NRMS, the RMS difference divided by the standard deviation of the observations in each $1/2^\circ$ longitude by $1/3^\circ$ latitude grid square) is also calculated (Figure 4). Model-observation comparisons for the ecosystem variables are calculated similarly using instantaneous data saved at daily frequency. Small values of the NRMS error indicate that the difference between model and observation is small compared to the variability of the observation in a $1/2^\circ$ by $1/3^\circ$ square. Values of NRMS < 0.5 represent very good agreement between model and observations; 0.5 – 1 is good; 1 – 2 fair; 2 – 3 poor and NRMS > 3 implies that the model has little skill in reproducing the observations. There is a geographical bias in the observations with the North Sea having the best coverage whilst other regions, such as the Celtic and Irish Seas, have only sparse nutrient data.

[23] Temperature is well represented in the model with average values of the NRMS error less than 0.5 over most of the region; the model results being slightly too cold compared to observations. The modeled salinity is generally too fresh with reasonable agreement with observations over much of the domain. Salinity errors are largest in the southern Irish Sea, the Celtic Sea, the English Channel, the Southern Bight of the North Sea and around the edge of the continental shelf. In most of these areas, the standard deviations of the observations are small resulting in large NRMS errors however, in the English Channel and Southern Bight of the North Sea, the model underestimates the salinity by ~ 1 – 1.5 . This most likely relates to difficulties in accurately modeling river plumes (particularly the vertical structure) at ~ 12 km model resolution. Using the ERSEM salinity parameterization of total alkalinity [Blackford and Gilbert, 2007], the salinity errors potentially translate to an underestimation of total alkalinity over most of the region, except for in the central Irish Sea, off the east coasts of England and Scotland, the North Sea south of $\sim 54.5^\circ$ N and the Kattegat, where the salinity errors could give rise to values of total alkalinity that are too large.

[24] Dissolved oxygen is well represented in the North Sea, while the modeled values show an overestimate westwards of the Bay of Biscay; the oxygen at depth is

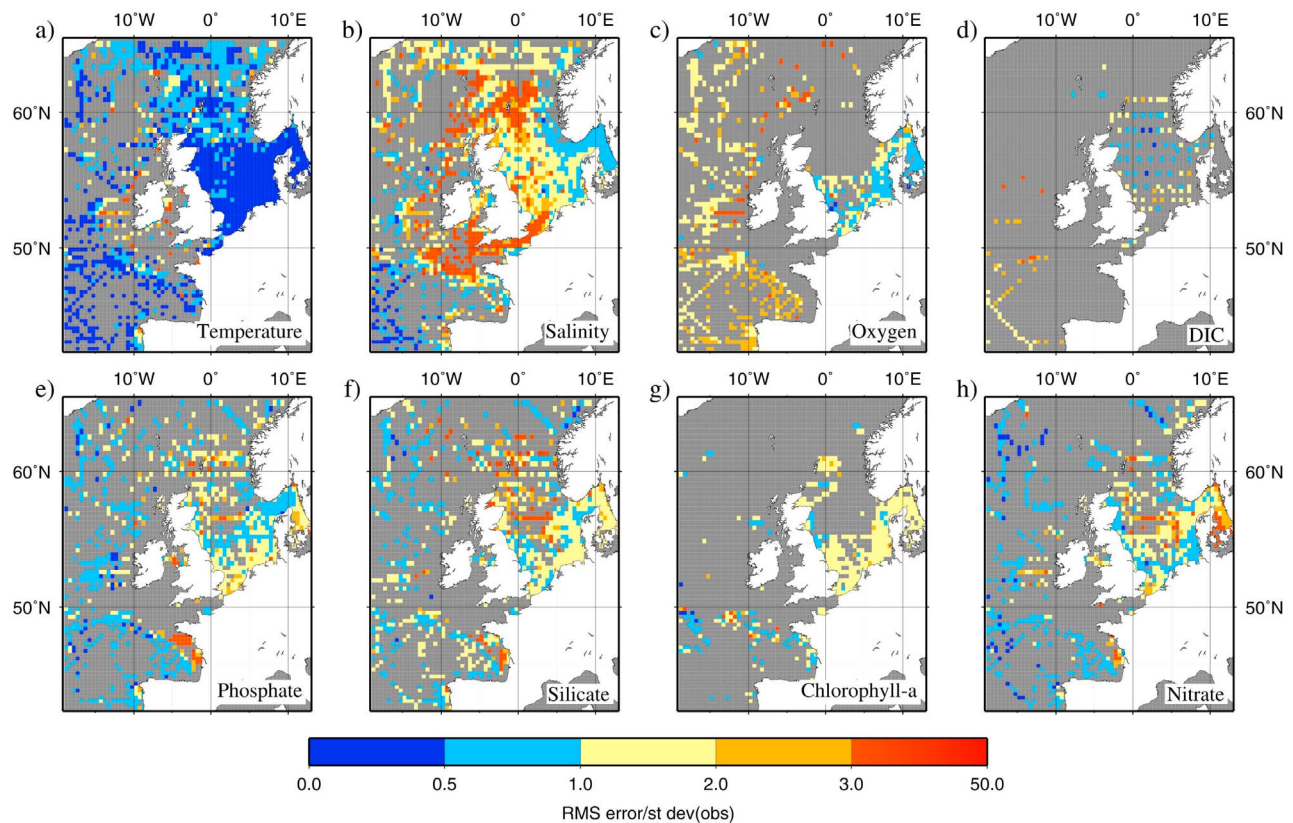


Figure 4. Normalized RMS errors (RMS difference/standard deviation of observations) for the model results compared to observations for (a) temperature, (b) salinity, (c) oxygen, (d) dissolved inorganic carbon (DIC), (e) phosphate, (f) silicate, (g) chlorophyll-a, and (h) nitrate. Values are averaged onto 1/2 by 1/3 degree squares.

$\sim 260\text{--}320\text{ mmol m}^{-3}$ in the model compared to observations of $\sim 240\text{--}260\text{ mmol m}^{-3}$ and the model fails to capture the observed oxygen minimum at $\sim 1000\text{ m}$. DIC has values of NRMS generally in the range 0.5–2 and is overestimated in the central (west-to-east) strip and coastal regions of the North Sea and underestimated in other regions of the North Sea and in the open ocean west of the Bay of Biscay. In regions where total alkalinity and DIC are either both overestimated (coastal regions of the central North Sea) or underestimated (the open ocean west of the Bay of Biscay and the northern North Sea) resulting errors in the calculated pCO_2 will tend to cancel. Elsewhere in the North Sea errors in total alkalinity and DIC are of opposite sign and will generate larger errors in pCO_2 . Phosphate is well represented in the open ocean, underestimated in the Irish Sea and in the southern and western North Sea and overestimated elsewhere, especially on the Armorican shelf, the Skagerrak and Kattegat. Silicate is less well modeled with values too low west of Biscay and in the southern and western North Sea and too high elsewhere; the NRMS errors are generally in the range 0.5–2. Chlorophyll-a data are rather sparse but show that the model underestimates chlorophyll-a in the southern North Sea, the Skagerrak and Kattegat and overestimates on the Armorican shelf; NRMS errors indicate reasonable agreement with observations. Nitrate tends to be slightly underestimated in the open ocean and overestimated on the shelf; NRMS errors show good agreement in the open ocean

and generally reasonable agreement on the shelf. In the central/southern North Sea the distribution of NRMS values among the model variables is similar to that found by *Allen et al.* [2007].

[25] Near surface (top 10 m of the water column) errors on seasonal timescales (Table 1) are determined using data from the World Ocean Database 2005, for the same parameters as in Figures 3 and 4. Mean (model – observations) and NRMS errors are calculated for 5 regions, aggregated from the regions shown in Figure 1. The largest mean errors occur in the oxygen, which is underestimated by the model near surface. For the surface nutrients, nitrate tends to be overestimated in the whole region, phosphate tends to be overestimated except in summer and autumn in the North Sea and throughout the year on the northwestern shelf and in the open ocean and silicate is underestimated during autumn and winter in the North Sea, the southwestern shelf and the open ocean and otherwise overestimated by the model. Mean temperature errors show that the model is generally too cold, except over the northwestern shelf and in the open ocean, while salinity is generally overestimated on the shelf and underestimated in the open ocean. On seasonal/regional scales, the NRMS errors in the top 10 m of the water column have values generally less than 2 for most parameters, showing that the model and observations are in good or fair agreement. Exceptions are the nutrients (especially nitrate) in the Skagerrak and Kattegat, DIC in the North Sea during

Table 1. Summary of the Mean Error (M = Model – Observation) and Normalized RMS (NRMS) Error in the Top 10 m of the Water Column, Calculated Over the Regions Shown in Figure 1^a

	Regions									
	1, 2, 3, 6		5		7, 8, 9		4, 10, 11		12, 13	
	M	NRMS	M	NRMS	M	NRMS	M	NRMS	M	NRMS
<i>Winter (December–February)</i>										
Oxygen	–29.2	1.3	–27.7	1.0					–20.1	2.5
Silicate	–4.1	0.9	2.0	1.1	0.3	0.9	–3.9	0.8	–0.5	1.0
Phosphate	0.1	1.2	0.3	1.8	–0.5	1.1	0.3	0.9	0.0	0.7
Nitrate	3.2	1.0	10.8	3.6	0.2	0.7	4.7	1.2	2.0	1.0
Chlorophyll-a	–1.1	1.1	–1.5	1.1	–0.2	3.1	0.1	1.0	–0.1	0.9
DIC	30.4	2.4								
Temperature	–0.4	0.6	–0.3	0.5	–0.5	0.9	–0.8	0.7	–0.3	0.3
Salinity	0.3	0.9	–0.1	0.6	0.2	0.5	0.7	0.8	0.0	1.0
pCO ₂	–27.6	1.3	8.4	2.6	–52.7	8.5	–14.6	0.8	–36.7	2.8
<i>Spring (March–May)</i>										
Oxygen	–31.7	1.4	–26.8	1.2	–30.9	1.7	–14.2	1.1	–17.1	1.4
Silicate	0.3	0.9	5.8	2.5	0.5	1.1	4.2	1.0	0.5	1.0
Phosphate	0.3	1.4	0.4	2.5	–0.2	1.1	0.0	0.9	0.0	0.9
Nitrate	3.3	1.2	7.5	2.4	–1.0	0.7	–0.2	0.9	–0.3	0.8
Chlorophyll-a	–4.3	1.1	–2.4	1.1	0.1	1.1	–2.5	1.1	0.0	2.0
DIC	18.9	1.3							–6.5	1.4
Temperature	–0.2	0.5	–0.3	0.3	0.1	0.5	–0.4	0.6	0.2	0.3
Salinity	0.2	0.8	0.8	0.6	0.2	0.5	0.4	0.9	–0.1	1.0
pCO ₂	–14.4	0.2	–53.2	1.6	–26.8	0.9	–18.3	0.5	–69.9	2.4
<i>Summer (June–August)</i>										
Oxygen	–16.0	1.1	–7.9	1.0					–31.6	1.0
Silicate	–0.8	1.0	4.5	3.0	0.9	1.6	–0.2	0.9	0.0	1.0
Phosphate	0.0	0.9	0.2	3.8	–0.7	1.3	0.0	1.0	–0.1	1.2
Nitrate	6.0	1.6	4.4	8.9	0.2	1.0	1.1	0.9	–0.9	1.0
Chlorophyll-a	–3.4	1.1	–1.1	1.0	–0.1	1.0	–1.9	1.1	–0.3	1.0
DIC	2.0	1.1							–62.9	2.5
Temperature	0.0	0.5	–0.5	0.7	1.2	1.5	0.4	0.5	1.0	0.4
Salinity	0.4	0.8	1.8	0.7	0.1	0.6	–0.3	1.0	–0.2	0.9
pCO ₂	–47.0	0.8	–53.1	1.0	–79.7	3.1	–40.7	0.9	–82.4	3.6
<i>Autumn (September–November)</i>										
Oxygen	–22.8	1.3	–25.0	1.3					–21.2	1.4
Silicate	–4.1	1.0	4.2	1.4	–1.3	1.0	–3.8	0.9	–0.6	1.0
Phosphate	–0.2	0.8	0.5	2.9	–0.3	1.1	0.0	1.0	–0.1	0.8
Nitrate	4.1	1.1	9.1	7.6	–0.5	0.7	0.2	0.9	0.1	0.9
Chlorophyll-a	–2.9	1.1	–2.4	1.2	–0.3	1.6	–1.1	1.0	0.0	1.2
DIC	8.5	1.6							–13.2	0.9
Temperature	–0.2	0.3	0.2	0.4	0.1	0.4	–0.2	0.3	0.0	0.2
Salinity	0.3	0.9	0.9	0.6	0.2	0.7	0.7	0.9	–0.1	1.0
pCO ₂	–70.2	1.4	17.6	0.4	–73.2	7.3	–58.8	1.7	–62.0	3.7

^aRegions: the North Sea and Norwegian Trench (1, 2, 3, and 6); the Skagerrak and Kattegat (5), the northwestern shelf and Irish Sea (7, 8, 9); the southwestern shelf (4, 10, and 11) and the open ocean (12 and 13). Errors in surface pCO₂ are also shown. Mean errors for oxygen, silicate, phosphate, nitrate and DIC are in mmol m^{–3}; for chlorophyll-a are in mg m^{–3}; for temperature in °C and for pCO₂ in μatm. The cells have been left blank where there are insufficient data corresponding to the season, region and parameter.

winter and in the open ocean during summer and oxygen in the open ocean during winter.

[26] From 1991 to 2004 for the study region there are over 400,000 observations of pCO₂ from the Surface Ocean CO₂ Atlas (SOCAT; <http://www.socat.info/access.html>) (B. Pfeil et al., A uniform, quality controlled, Surface Ocean CO₂ Atlas (SOCAT), Earth System Science Data, manuscript in preparation, 2012). The mean and NRMS errors for surface pCO₂ integrated over 5 regions are shown in Table 1. Errors in pCO₂ are expected to be large since errors in the salinity and DIC and in the parameterizations will all contribute [Artoli et al., 2012]. On average, the model underestimates pCO₂ everywhere except in the Skagerrak and Kattegat during autumn and winter. NRMS errors are

generally higher in the autumn and winter, with poor agreement between model and observations in the Skagerrak/Kattegat and on the northwestern shelf, NRMS errors are also high in the open ocean. NRMS errors show good to fair agreement between model and observations in the North Sea and the southwestern shelf as a result of the high variability of the observations in these regions.

4. Carbon Budgets and Fluxes

4.1. Analysis

[27] Organic and inorganic carbon budgets are calculated from the model simulations by considering the conservation of mass, taking into account that the volume varies in time

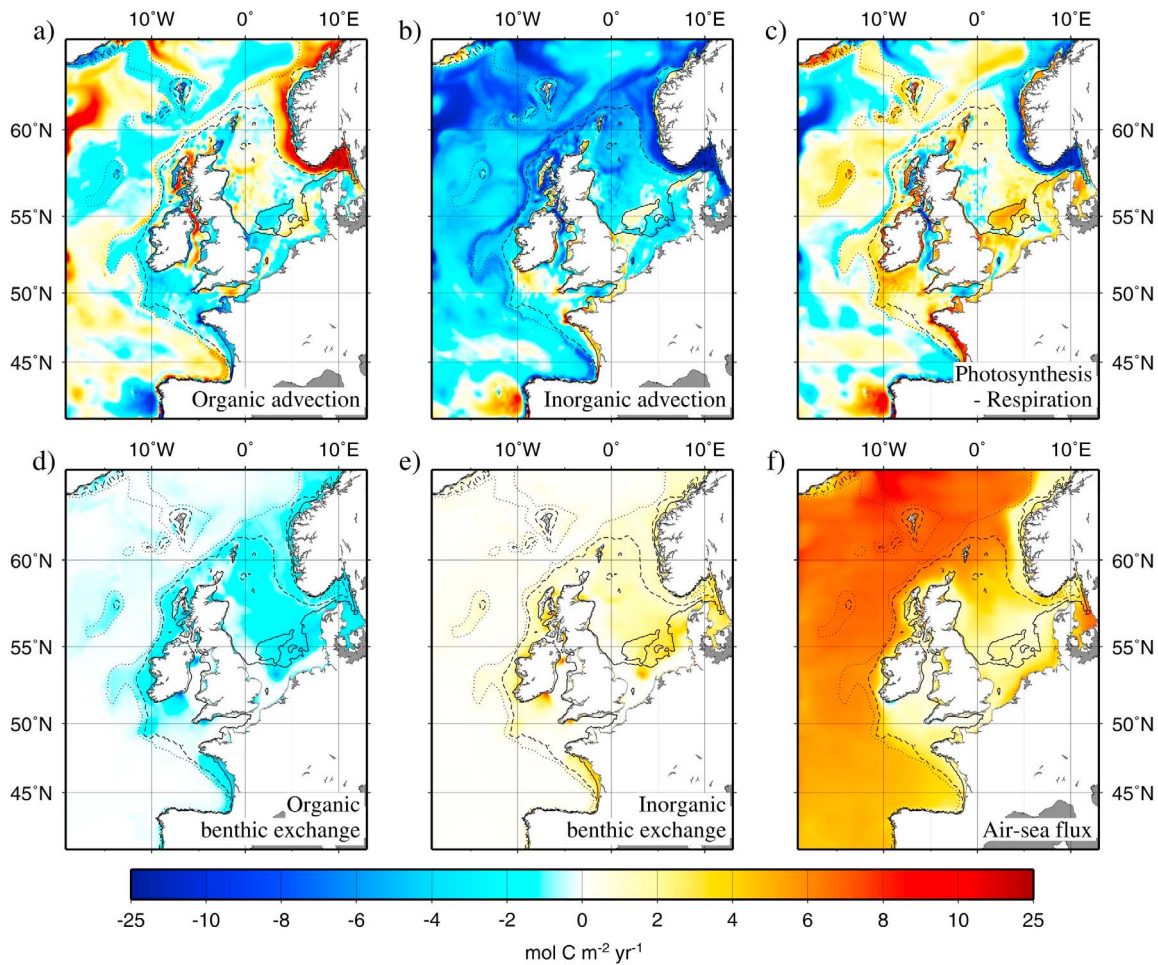


Figure 5. The carbon budget densities averaged over 1989 to 2004: (a) the advection of organic carbon, (b) the advection of inorganic carbon, (c) the net carbon uptake (gross photosynthesis minus community respiration), (d) the pelagic-benthic exchange of organic carbon (negative is loss from the pelagic system), (e) the pelagic-benthic exchange of DIC (positive is gain to the pelagic system), and (f) the air-sea flux (positive is CO_2 uptake by the ocean). The solid, dashed, and dotted lines represent the 40, 150, and 500 m isobaths, respectively.

with the sea level. The equations for changes in the volume-integrated inorganic/organic carbon mass, $C_{i,o}$, are

$$\frac{dC_i}{dt} = F_i + F_A - PR + R_{ben} + R_i \quad \text{mol C yr}^{-1} \quad (3)$$

$$\frac{dC_o}{dt} = F_o + PR + S_{ben} + R_o \quad \text{mol C yr}^{-1} \quad (4)$$

where C_i is the DIC mass and C_o the total organic carbon content comprising phytoplankton, zooplankton, detritus and bacteria. The amount of inorganic carbon provided by the rivers, R_i , is calculated using river flow rates and the river DIC concentrations, while the organic river contribution, R_o , is calculated from river flows and model values of POC and DOC in outflow boxes. The other terms are: F_i and F_o , the advective fluxes of the inorganic and organic carbon; F_A , the air to sea carbon flux; PR , the difference between gross primary production and total community respiration; R_{ben} , the DIC flux from benthos; S_{ben} , the net organic carbon flux between the benthic and pelagic models (due to the balance

between settling and resuspension of particulate carbon and benthic feeding on phytoplankton). These terms are calculated at each ERSEM time step (every 1200 s) and output as seven-day means. The advective flux and net photosynthesis terms are then integrated vertically over the water column. At this stage, the carbon terms are horizontally-resolved ‘densities’ (see Figure 5). To complete the budget in equations (3) and (4), each term is integrated horizontally over the regions shown in Figure 1. By integrating over 16 years, the effect on the calculations of any changes in water volume due to short-period disturbances such as tides and surges is negligible.

[28] The standard deviation of the annual means of the DIC flux from the benthos, R_{ben} , in regions 12 and 13 reduced by 85% for 1989–2004, compared to the value for 1984–2004, indicating that errors due to uncertainties in the initial conditions are significantly reduced after five years of model spin-up.

4.2. Results

[29] The 16-year mean depth-integrated carbon budget advection terms are shown in Figures 5a and 5b. Both

organic and inorganic advection have largest magnitudes in the slope current and the Norwegian coastal current demonstrating an increase in organic carbon and a decrease in inorganic carbon in these regions. The two advection components are strongly anti-correlated as photosynthesis and respiration exchange carbon between the organic and inorganic pools while CO₂ uptake from the atmosphere is an additional factor in the inorganic advection (see below).

[30] The mean total pelagic community respiration (from phytoplankton, zooplankton and bacteria) largely balances the photosynthesis (Figure 5c) but there is significant net carbon uptake (autotrophy) in the shallower regions of the North Sea and to the south of Ireland, around the Faroe Islands and on Rockall Bank. The Norwegian Trench, the northwestern North Sea and parts of the shelf break from north of Ireland to Scotland are areas where respiration exceeds photosynthesis and there is a net flux of carbon from organic to inorganic (heterotrophy). This is balanced by the transport of organic carbon into the Norwegian Trench from the North Sea and along the shelf break from the Celtic Sea/Goban Spur, with corresponding transport of inorganic carbon out of these regions.

[31] On the shelf, the difference between the rates of erosion at the sea bed and the loss of pelagic carbon by deposition and benthic feeding (Figure 5d) acts to remove organic carbon from the pelagic system. The largest rates of removal are around the south coast of Ireland, the west coasts of Ireland, Scotland and France and south and east of Dogger Bank in the North Sea. The exchange of inorganic carbon between the pelagic and benthic systems (Figure 5e) is due to a diffusive flux of DIC from the benthic to the pelagic system. In the North Sea, there is a net gain of carbon from the benthos of $0.006 \pm 0.015 \times 10^{12} \text{ mol C yr}^{-1}$. The model flux represents a small loss from the benthos amounting to $0.3\% \text{ yr}^{-1}$ of the initial benthic carbon in the North Sea; small compared to the standard deviation of the annual mean flux.

[32] With some small exceptions (areas to the south of Ireland and to the southwest of England), the north east Atlantic is a region of CO₂ uptake from the atmosphere (Figure 5f). Away from the shelf, net uptake is $\sim 4\text{--}6 \text{ mol C m}^{-2} \text{ yr}^{-1}$, rising to $\sim 6.5\text{--}7.5 \text{ mol C m}^{-2} \text{ yr}^{-1}$ in the Rockall Trough, around the Faroe Islands, across the Faroe-Shetland channel and over the Wyville-Thomson ridge, about twice the values of $0.7\text{--}3.5 \text{ mol C m}^{-2} \text{ yr}^{-1}$ given by *Takahashi et al.* [2009] for the eastern North Atlantic. There are similar values along the shelf break and following the inflow of Atlantic water into the North Sea. Away from the shelf break, the largest air-sea fluxes on the shelf occur in the southern and eastern regions of the North Sea and the coastal areas of the eastern Irish Sea. The Celtic Sea and Irish Sea have lower uptake of CO₂. The model suggests an annual uptake of $2.1 \text{ mol C m}^{-2} \text{ yr}^{-1}$ in the Celtic Sea and $2.6 \text{ mol C m}^{-2} \text{ yr}^{-1}$ on the Armorican shelf, in fair agreement with the observations of *Frankignoulle and Borges* [2001], who estimate CO₂ flux in the Celtic Sea and Bay of Biscay as being between 1.7 and $2.9 \text{ mol C m}^{-2} \text{ yr}^{-1}$. Modeling studies on the American continental shelf in the western North Atlantic [*Fennel and Wilkin*, 2009; *Fennel*, 2010] show that the area-normalized air-sea flux of CO₂ is not significantly larger on the shelf regions than in the adjacent deep ocean. For the European shelf the CO₂ uptake (Figure 5f) is larger over the deep oceans and continental slopes than over most of the shelf

region. High CO₂ uptake over the deep ocean partially drives the negative advection of inorganic carbon here (Figure 5b) as the DIC is transported away.

[33] Using data from cruise tracks predominately along the centre of the English Channel, *Borges and Frankignoulle* [2003] state that this area is probably neutral in terms of air-sea flux of CO₂. The model results show a region of low CO₂ uptake ($\sim 0.2\text{--}0.8 \text{ mol C m}^{-2} \text{ yr}^{-1}$) along the English Channel centre but with larger values near the coasts, except for a small region of outgassing along the southwest coast of England.

[34] The model results are in qualitative agreement with *Schiettecatte et al.* [2007] who use high frequency observations in the Southern Bight of the North Sea to show that the region is a sink for atmospheric CO₂, of the order of $0.7 \text{ mol C m}^{-2} \text{ yr}^{-1}$. In contrast, the CO₂ flux calculated from observations by *Thomas et al.* [2004] show out-gassing in the Southern Bight. In the northern North Sea, both model and observations [*Thomas et al.*, 2004] show an increased CO₂ uptake towards the Fair Isle channel. The total CO₂ uptake from the atmosphere for the North Sea (regions 1, 2, 3 and 6 in Figure 1) is $1.5 \times 10^{12} \text{ mol C yr}^{-1}$, compared to values of $0.7 \times 10^{12} \text{ mol C yr}^{-1}$ and $0.8 \pm 0.1 \times 10^{12} \text{ mol C yr}^{-1}$ estimated from spatial surveys and budgets by *Thomas et al.* [2004, 2005a].

[35] Mean annual cycles of the carbon budget density terms (Figure 6) at six points on the continental shelf show broadly similar behavior. In all cases, the net photosynthesis dominates the other terms, with uptake of DIC into organic carbon strongest during spring and early summer and respiration of organic carbon to DIC dominating during autumn and winter. The advection terms oscillate between increasing and decreasing the carbon pools, except in the southern North Sea and the Armorican Shelf, where advection removes organic carbon, and in the northern North Sea, where advection removes inorganic carbon throughout the year. The inter-annual variability of the monthly mean carbon budget terms, as represented by the error bars showing the standard deviations, is largest for the advection terms. This is because advection is the term most affected by changes in sea level and it shows the importance of using long time series to study oceanic budgets. Carbon exchange with the benthos is small, particularly in the southern North Sea and the English Channel, although the benthic DIC flux is of similar magnitude to the air-sea flux in the central North Sea, the Celtic Sea and the Armorican Shelf. At all points, the air-sea CO₂ flux exhibits outgassing or relatively low levels of ingassing in the winter, strong ocean uptake during the spring bloom (April to May), followed by a period of lower uptake before a second, smaller, peak in late summer. In contrast to observations [*Schiettecatte et al.*, 2007], the model predicts CO₂ uptake throughout the year at the point in the southern North Sea.

[36] The terms of the carbon budget, time integrated over 16 years and spatially integrated over each region in Figure 1, are shown in Figure 7. The results show a complex interplay between the biological processes, advection and exchange with the benthic sub-model; there is no simple relation, region by region, between photosynthesis and CO₂ draw down. In the organic budget, the net uptake of carbon through the difference between photosynthesis and respiration (the increase in the organic carbon pool) is largely

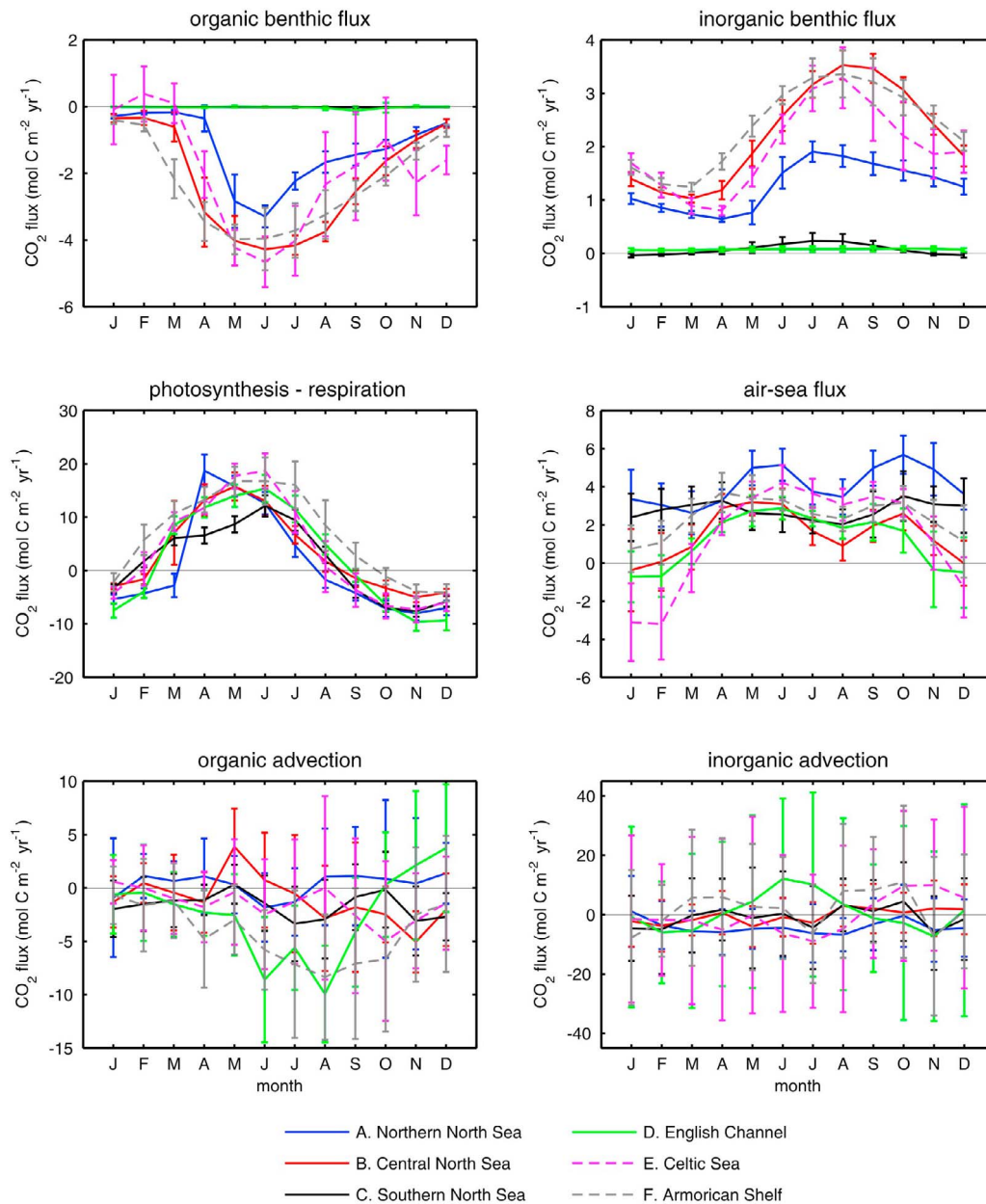


Figure 6. Mean annual cycles (1989 to 2004) of the carbon budget density terms for the six locations (A–F) shown in Figure 1. Except for in the photosynthesis-respiration term (representing conversion of inorganic carbon to organic carbon), positive (negative) values denote increase (decrease) in the amount of carbon in the water column. The error bars are standard deviations of the monthly mean values over the 16-year simulation.

balanced by losses due to settling and advection. Only in the Norwegian Trench and the Skagerrak/Kattegat is the spatially averaged photosynthesis-respiration term negative and this is balanced by an influx of organic carbon. In the inorganic budget, the reduction of inorganic carbon through advection and the excess of photosynthesis over respiration are largely balanced by diffusion of DIC from the benthos, CO_2 uptake from the atmosphere and input of DIC from rivers and the Baltic. Except for the open ocean regions, the tendency term (the change in total carbon content) is small compared with the other terms, indicating that the model is largely close to equilibrium, and not drifting significantly

over the 16 years of the model simulation. The two open ocean sectors, 12 and 13, have larger positive trends in the inorganic carbon budget due to an excess of in-gassing of CO_2 over the losses due to advection and the difference between respiration and photosynthesis. Some increase in the total carbon content is expected since the atmosphere-ocean system is out of equilibrium due to increasing levels of atmospheric CO_2 from anthropogenic sources and the equilibrium time of the deep ocean exceeds the run length considered here.

[37] The advection terms have the highest inter-annual variability (denoted by the error bars in Figure 7) particularly

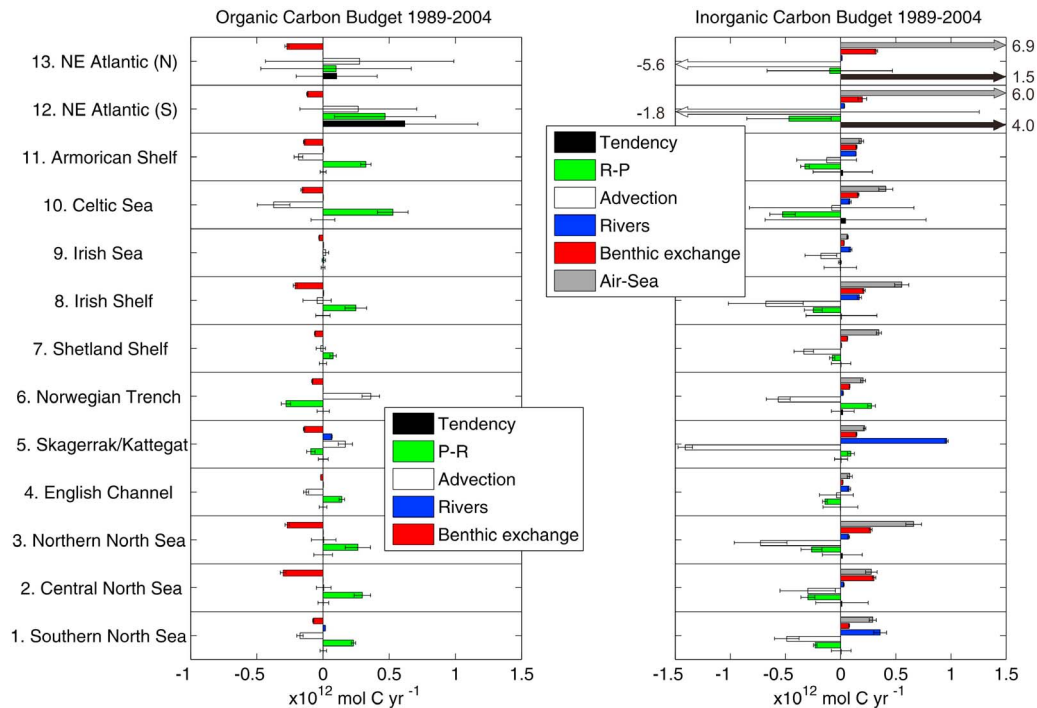


Figure 7. The terms of the carbon budget for regions of the northeast Atlantic (Figure 1) separated into (a) organic and (b) inorganic components. The organic budget is divided into the organic tendency, net uptake through photosynthesis (P-R), horizontal advection, input from rivers and net settling from the pelagic system to the benthos (benthic flux), while the inorganic budget comprises the inorganic tendency, net loss through photosynthesis (R-P), horizontal advection, input from rivers, benthic flux and uptake of CO_2 from the atmosphere. The contributions from the Baltic are included in the river terms. The error bars are standard deviations of the annual budget terms.

in the Celtic Sea and on the Irish Shelf. For the inorganic carbon budget, the variability of the trend in C_i (the tendency) is close to the variability of the inorganic advection indicating that the variability of the advection is strongly influencing that of the trend in C_i . The inter-annual variabilities of the air-sea flux and the net photosynthesis are of approximately the same order, but much smaller than those of the advection and trend in C_i . In the organic budget, the variability of the net photosynthesis is close to, but smaller, than that of advection, closely followed by the variability of the trend in C_o , indicating a much closer relationship between the variabilities of these terms in the organic budget than in the inorganic budget. River sources and benthic fluxes have the smallest inter-annual variabilities.

[38] Changes in the volume of the model due to the movement of the free surface over the 16-year period do not significantly affect the carbon budgets in Figure 7. In the inorganic budget, for example, assuming a constant concentration for DIC of $2100 \text{ mmol C m}^{-3}$, the volume changes in the 13 regions give rise to rates of carbon change of between $-0.06 \times 10^{12} \text{ mol C yr}^{-1}$ (for region 13) and $0.02 \times 10^{12} \text{ mol C yr}^{-1}$ (for region 3), accounted for in the tendency term in Figure 7.

[39] Budgets for the North Sea, the whole northwest European continental shelf and the open ocean are obtained (Table 2) by integrating the carbon budget terms (Figure 7) over those regions. For the shallower areas – the North Sea and the European shelf – the settling of organic carbon to the

benthos is closely balanced by the benthic flux of DIC. For the North Sea, the CO_2 uptake, the river and Baltic inflows and the net transport of organic carbon into the area are balanced by the horizontal transport of inorganic carbon out of the area, which occurs mainly via the Norwegian Trench. The budget for the North Sea is in qualitative agreement with that of Thomas *et al.* [2005a], although the model uses smaller inputs of river carbon and estimates higher CO_2 uptake from the atmosphere. Both studies agree that the net transport of organic/inorganic carbon is into/out of the region and that there is net conversion of organic carbon to DIC of $\sim 0.3 \times 10^{12} \text{ mol C yr}^{-1}$ [Thomas *et al.*, 2005a] and $\sim 0.2 \times 10^{12} \text{ mol C yr}^{-1}$ (from modeled benthic-pelagic fluxes and differences between community respiration and photosynthesis).

[40] For the European shelf as a whole (Table 2), the uptake of CO_2 from the atmosphere and input of DIC/DOC from rivers and the Baltic are offset by the net flux of both organic and inorganic carbon off the shelf into deeper waters.

[41] In the open ocean, the model shows a mean increase in both organic and inorganic carbon over the 16 years of the simulation but with high inter-annual variability (standard deviations). In the ERSEM benthic model, POC in the open ocean is lower and bacteria concentrations are higher than values derived by Rowe and Deming [1985] from observations in the Bay of Biscay. This suggests that bacterial activity is overestimated by the model, leading to a reduction in benthic POC and allowing too much DIC to be released into the water column. Of the other carbon budget terms,

Table 2. Summary of Average Values of the Carbon Budget Terms ($\times 10^{12}$ mol C yr⁻¹) Integrated Over the Open Ocean (Regions 12 and 13 in Figure 1), the European Shelf (Regions 1–11), and the North Sea (Regions 1, 2, 3, and 6) for 1989–2004 and the Standard Deviations of the Annual Mean Fluxes^a

	Open Ocean		European Shelf		North Sea		Thomas <i>et al.</i> [2005a]
	Mean	st dev	Mean	st dev	Mean	st dev	
<i>Inorganic Carbon</i>							
Tendency	5.5	3.8	0.1	1.2	0.1	0.4	
Respiration – photosynthesis	–0.6	0.7	–1.7	0.3	–0.5	0.2	0.3 ^b
Advection	–7.4	3.4	–5.5	1.2	–2.0	0.5	–1.9
River input	0.0	0.0	2.6	0.1	0.4	0.1	0.8
Benthic flux	0.5	0.1	1.5	0.1	0.7	0.0	
Air-sea flux	12.9	0.7	3.3	0.2	1.4	0.1	0.8
<i>Organic Carbon</i>							
Tendency	0.7	0.8	0.0	0.3	0.0	0.1	
Photosynthesis – respiration	0.6	0.7	1.7	0.3	0.5	0.2	–0.3 ^c
Advection	0.5	0.9	–0.4	0.4	0.2	0.1	0.3
River input	0.0	0.0	0.1	0.0	0.0	0.0	0.1
Benthic flux	–0.4	0.0	–1.5	0.1	–0.7	0.0	–0.07

^aThe river values include input from the Baltic. Carbon budget terms for the North Sea from Thomas *et al.* [2005a] are also included.

^bFor net heterotrophy, represented in the model by the sum of benthic exchange and difference between respiration and photosynthesis.

^cFor net heterotrophy, represented in the model by the loss of carbon to the benthos by settling plus the net uptake by photosynthesis.

there is a large flux from the atmosphere to the sea while advection and the settling of organic carbon are acting to remove carbon from the region.

[42] In order for off-shelf advection to be an effective mechanism for the removal of carbon from interaction with the atmosphere, the carbon must be transported to below the level of the permanent pycnocline in the North Atlantic. For this to be possible, the off-shelf transport of carbon must occur in the lower part of the water column. Water volume and carbon fluxes between the open ocean and the shelf across the 200 m depth contour adjoining regions 7, 8, 10 and 11 (Figure 1) and across 60.833°N through the Norwegian Trench (adjoining region 6 in Figure 1) are shown in Table 3. Since much of the off-shelf transport occurs in a narrow lower Ekman layer below 180 m deep [Holt *et al.*, 2009], the transports are divided into two layers – an upper layer in the top 180 m of the water column and a lower layer below 180 m. In the following discussion, standard deviations of annual mean values are used to represent uncertainties in transported quantities; when integrating values along several sections or through the water column the uncertainties are calculated from annual means of the integrated quantities. The total transports of water (1.34 ± 0.13 Sv) and carbon ($94 \pm 9 \times 10^{12}$ mol C yr⁻¹) out through the Norwegian

Trench are in fair agreement with the model estimates of 1.52–1.6 Sv and $105\text{--}111 \times 10^{12}$ mol C yr⁻¹ calculated by Kühn *et al.* [2010] for 1995 to 1996. The volume fluxes in the two layers show the downwelling circulation of the north-west European shelf [Holt *et al.*, 2009], with average fluxes being towards the shelf in the upper layer and towards the open ocean in the lower layer. POC and DIC are transported from the open ocean onto the shelf in the upper layer along the shelf break from the Celtic Sea to northeast of Scotland. Elsewhere, carbon in the upper layer is transported towards the open ocean with the largest fluxes being in the Norwegian Trench. In the bottom 20 m of the water column of the regions adjacent to the shelf edge, a small amount of DIC is upwelled onto the Armorican shelf but the predominant direction of carbon transport is from the shelf to the open ocean, with the largest fluxes being from regions 7 and 8 (northeast of Scotland to west of Ireland). In the lower layer in the Norwegian Trench, carbon is also transported towards the open ocean. The net carbon transport is $112 \pm 21 \times 10^{12}$ mol C yr⁻¹ onto the shelf in the top 180 m and $118 \pm 21 \times 10^{12}$ mol C yr⁻¹ off the shelf below 180 m, giving a net flux off shelf of $6 \pm 1 \times 10^{12}$ mol C yr⁻¹ which amounts to ~3% of the global export flux (assuming a global ocean uptake of 2.2 Gt C yr⁻¹ [Le Quéré *et al.*, 2009]). Both

Table 3. Mean Ocean-Shelf Transports of Organic Carbon, Inorganic Carbon, and Water to Regions 6 (the Norwegian Trench), 7 (the Shetland Shelf), 8 (the Irish Shelf), 10 (the Celtic Sea), and 11 (the Armorican Shelf) (Figure 1) Averaged Over 1989–2004^a

Region	Organic C Flux ($\times 10^{12}$ mol C yr ⁻¹)				Inorganic C Flux ($\times 10^{12}$ mol C yr ⁻¹)				Volume Flux (Sv)			
	Upper Layer		Lower Layer		Upper Layer		Lower Layer		Upper Layer		Lower Layer	
	Mean	st dev	Mean	st dev	Mean	st dev	Mean	st dev	Mean	st dev	Mean	st dev
6	–1.0	0.1	–0.1	0.0	–78.9	6.6	–13.9	5.7	–1.14	0.10	–0.20	0.08
7	0.5	0.1	–0.1	0.0	64.3	4.9	–22.0	1.7	0.96	0.07	–0.33	0.03
8	1.0	0.2	–0.2	0.0	127.9	23.6	–77.5	15.8	1.90	0.35	–1.15	0.24
10	0.1	0.2	–0.0	0.0	22.3	15.4	–5.0	5.6	0.33	0.23	–0.07	0.08
11	–0.6	0.2	–0.0	0.0	–23.5	15.6	0.9	5.1	–0.35	0.23	0.01	0.08
Total	–0.0	0.4	–0.3	0.1	112.1	21.1	–117.5	21.3	1.70	0.32	–1.74	0.32

^aStandard deviations are calculated from the annual mean fluxes. Transports are divided into an upper layer (above 180 m) and a lower layer (below 180 m) and positive values denote transport from the open ocean. 1 Sv = 10^6 m³ s⁻¹.

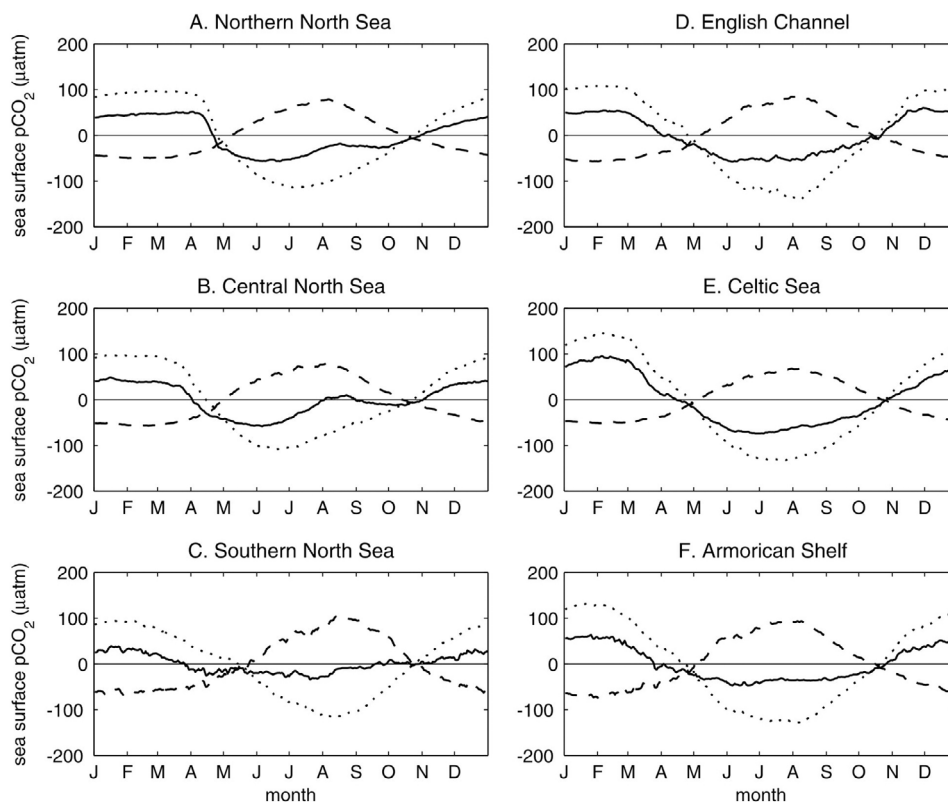


Figure 8. Mean annual cycles (1989 to 2004) of the sea surface $p\text{CO}_2$, relative to a mean value; $p\text{CO}_{2,\text{ref}}$ from the reference simulation (solid lines), $p\text{CO}_{2,\text{temp}}$ from temperature variations (dashed lines) and $p\text{CO}_{2,\text{bio}}$ from biological effects (dotted lines) for the six locations (A–F) shown in Figure 1.

the downwelling circulation of the shelf and the biological carbon pump contribute to the net off-shelf transport of carbon. An estimate of their relative contributions may be obtained by assuming that biological processes are not present and that carbon is homogeneously distributed. Then, in the top 180 m of the water column, the on-shelf volume flux of 1.70 Sv, transporting $112 \times 10^{12} \text{ mol C yr}^{-1}$, would be associated with an off-shelf transport of $115 \times 10^{12} \text{ mol C yr}^{-1}$ below 180 m depth, due to the volume flux of 1.74 Sv. This simple estimate suggests that both the biological carbon pump and the large scale circulation are significant processes leading to net off-shelf transport of carbon. Of the off-shelf carbon transport, $104 \pm 16 \times 10^{12} \text{ mol C yr}^{-1}$ occurs in the top 180 m of the water column and $119 \pm 23 \times 10^{12} \text{ mol C yr}^{-1}$ below that depth, therefore more than half of the off-shelf transport of carbon takes place in the lower layer. Given that the permanent pycnocline generally lies below 180 m, this represents an upper bound on the percentage of carbon removed from atmospheric exchange on centennial timescales.

5. Controls on $p\text{CO}_2$

[43] The air-sea exchange of CO_2 is determined by the difference between the partial pressure of CO_2 in surface waters and in the overlying atmosphere. Seasonal and geographic variations in atmospheric $p\text{CO}_2$ tend to be much smaller than those of surface water $p\text{CO}_2$. Data averaged from observations at the Azores, Mt Cimone and Mace Head

(J. Remedios and R. Leigh, personal communication, 2007), used here for model forcing, vary between 350 and 380 ppmv from 1989 to 2004, while surface water $p\text{CO}_2$ calculated from POLCOMS-ERSEM has a mean annual range at a point of $\sim 100 \mu\text{atm}$ and a mean range over the domain of $\sim 500 \mu\text{atm}$. The higher variability of surface water $p\text{CO}_2$ implies that it is the dominant quantity governing the direction and magnitude of the air-sea CO_2 flux. The $p\text{CO}_2$ in surface water is affected by seasonal and spatial changes in temperature, DIC concentration and alkalinity.

[44] The relative importance of temperature and biology in controlling $p\text{CO}_2$ is estimated by comparing the POLCOMS-ERSEM simulation described above with the results of a repeat simulation with biological processes omitted in the calculation of DIC. In the second simulation, DIC depends on water temperature, the air-sea flux of CO_2 , riverine DIC outflows and advection only; changes due to photosynthesis, respiration and diffusion from the benthos are not included. The effect of biological processes on the surface water $p\text{CO}_2$ is then defined by $p\text{CO}_{2,\text{bio}} = p\text{CO}_{2,\text{ref}} - p\text{CO}_{2,\text{temp}}$, where $p\text{CO}_{2,\text{ref}}$ is from the original (reference) simulation and $p\text{CO}_{2,\text{temp}}$ is from the simulation without biological processes. This method for separating the physical and biological signals of $p\text{CO}_2$ gives comparable results to the method used by Takahashi *et al.* [2002] for observed data in the global ocean, but with the benefit that the effects of advection are explicitly included.

[45] Average annual cycles for $p\text{CO}_{2,\text{bio}}$, $p\text{CO}_{2,\text{ref}}$ and $p\text{CO}_{2,\text{temp}}$ are calculated for 1989 to 2004. For ease of

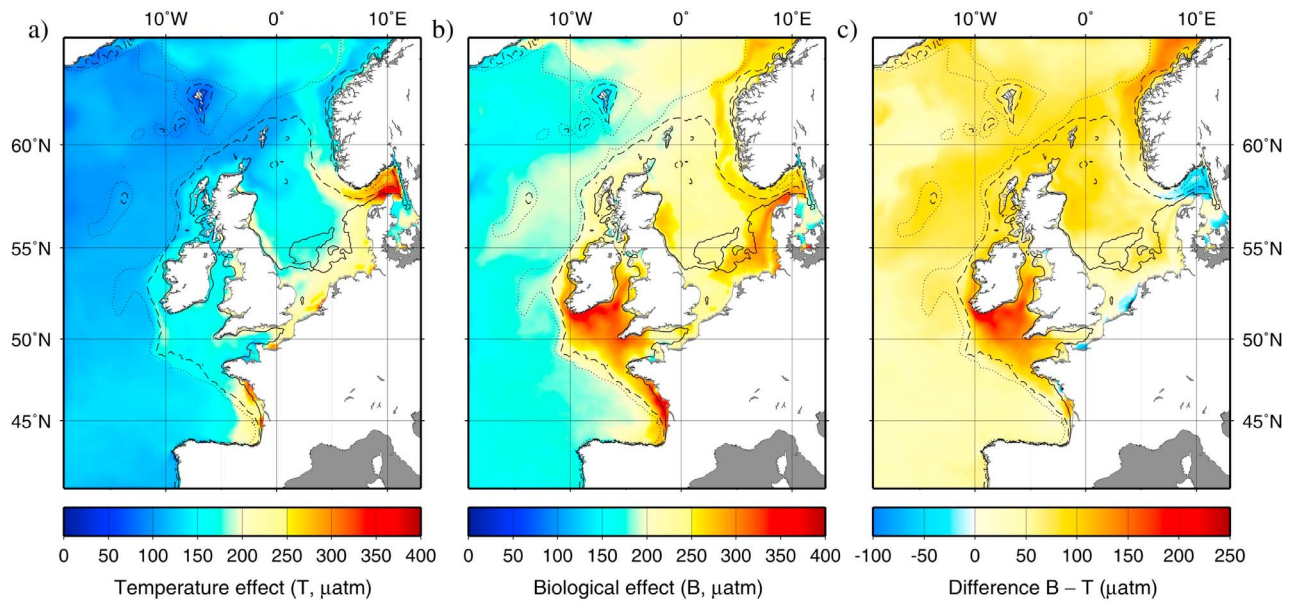


Figure 9. The annual $p\text{CO}_2$ amplitude due to (a) the temperature effect and (b) the biological effect and (c) the difference between the biological and temperature effects, all averaged over 1989–2004. The solid, dashed, and dotted lines represent the 40, 150, and 500 m isobaths, respectively.

comparison, and since we are interested in the relative amplitudes of the $p\text{CO}_2$ signals, the mean value is subtracted from each average time series. For the six points (A–F, Figure 1), the behaviors of the $p\text{CO}_2$ time series are broadly similar (Figure 8). Values of $p\text{CO}_{2,\text{ref}}$ are largest in the winter, reduce in the spring before increasing again in late autumn. At the points in the central and northern North Sea, there is a late summer peak in $p\text{CO}_{2,\text{ref}}$ levels. The largest mean range of $p\text{CO}_{2,\text{ref}}$ ($169 \mu\text{atm}$) occurs in the Celtic Sea while the smallest ($73 \mu\text{atm}$) is in the southern North Sea. This is in contrast to field measurements [Borges *et al.*, 2006] which show higher seasonal amplitudes in the southern North Sea. The model chlorophyll-*a* values are smaller than those observed in the southern North Sea indicating that there may be too little production here, resulting in an underestimate of the $p\text{CO}_2$ amplitude. Both the temperature and biological effects have a strong seasonal signal but are out of phase with one another. The temperature contribution to $p\text{CO}_2$ is a minimum in late winter, increasing to a peak in late summer before decreasing towards autumn. On the continental shelf the strength of the temperature effect on $p\text{CO}_2$ is related to the water depth, being largest in the shallower water of the southern North Sea (a mean annual range of $171 \mu\text{atm}$ in 25 m of water) and smallest in the Celtic Sea (mean annual range of $121 \mu\text{atm}$ in 100 m of water). The biological contribution is a maximum in the winter, decreasing rapidly in spring (as DIC is taken up in the production of organic matter) to a summer minimum before increasing with the onset of autumn (as DIC is released back into the water column). The strongest biological effects occur in the Celtic Sea, with a mean annual range of $278 \mu\text{atm}$, while the time series in the North Sea have the smallest ranges of 207 – $212 \mu\text{atm}$. Using data from observations, Thomas *et al.* [2005b] estimate the average biological signal for the North Sea to be $160 \mu\text{atm}$ and the average temperature signal to be $130 \mu\text{atm}$. Here, averaging values from the model at points A, B and C gives

a biological range of $210 \mu\text{atm}$ and a temperature range of $146 \mu\text{atm}$.

[46] Average amplitudes of the temperature, $T = \max(p\text{CO}_{2,\text{temp}}) - \min(p\text{CO}_{2,\text{temp}})$, and biological, $B = \max(p\text{CO}_{2,\text{bio}}) - \min(p\text{CO}_{2,\text{bio}})$, signals are calculated for each model point (Figure 9). In the northeastern Atlantic, the amplitude of the biological effect on $p\text{CO}_2$ dominates over that of the temperature. The difference is largest over the western shelf regions, the northwestern North Sea and the northern Norwegian Trench, with B exceeding T by 80 – $200 \mu\text{atm}$. This is due to a combination of the generally higher biological production on the shelf compared to open ocean values and the reduced seasonal range of surface temperatures (and hence T) in these deeper regions of the shelf. For the North Sea, the value of $B-T$ ranges from $\sim 50 \mu\text{atm}$ over Dogger Bank to $\sim 70 \mu\text{atm}$ in the central northern North Sea and $\sim 110 \mu\text{atm}$ in the northwest, in qualitative agreement with Thomas *et al.* [2005b], who also show that $B-T$ increases to the north and west. However, except near the coast in the south, we find that the biological effect on $p\text{CO}_2$ dominates throughout the North Sea, whereas Thomas *et al.* [2005b] find that the temperature effect dominates to the south of Dogger Bank. Both studies agree that the amplitude of the temperature effect is $\sim 200 \mu\text{atm}$ in the southern North Sea and $\sim 100 \mu\text{atm}$ in the north and that the biological effect is stronger in the northern than in the central North Sea; the discrepancy in $B-T$ in the south is due to differences in the amplitude of the biological signal (~ 220 – $260 \mu\text{atm}$ in this study compared to 100 – $150 \mu\text{atm}$ in Thomas *et al.* [2005b]). Using the MIRO-CO2 model in the Belgian Coastal Zone of the Southern Bight, Gypens *et al.* [2004] calculate that biological activity has a stronger influence than temperature on the seasonal cycle of $p\text{CO}_2$, in agreement with the assessment by Schiettecatte *et al.* [2006] based on observations in this region and the POLCOMS-ERSEM results presented here. In the open ocean, $B-T$ varies from

~40 μatm (in the south) to ~80 μatm (in the north), in agreement with values of 15–90 μatm estimated from observations by Takahashi *et al.* [2002] for this region.

6. Conclusions

[47] We present an estimated carbon budget for the European continental shelf and the adjacent North Atlantic Ocean derived from a multi-year simulation of POLCOMS-ERSEM. The model results give a useful understanding of the system and are an important step in quantifying the carbon budget of this region. A particular benefit of using a model to study the carbon budget is to demonstrate areas of sensitivity in the system. It is clear that estimates of a regional carbon budget depend on a number of closely matching balances. Several of the components of the carbon budget also exhibit high inter-annual variability (Figures 6 and 7) demonstrating the need to employ multi-year model simulations or observational data sets. The largest and most variable term in the modeled carbon budget is the advection of inorganic carbon, accurate estimation of which requires precise representation of the vertical profiles of both horizontal transport and DIC, particularly at the land-sea and shelf-ocean interfaces. The simulation accounts for the high degree of spatial and temporal heterogeneity of the carbon budget in the northeast Atlantic, processes that are significantly under sampled by observational programmes.

[48] The seasonal cycle of pCO_2 in sea water depends on water temperature and biological processes and the model suggests that, in this region of the northeast Atlantic, the biological effect is dominant and hence has the larger effect on the air-sea flux of CO_2 . The modeled air-sea fluxes are in qualitative agreement with several published values estimated from observations, although there is a tendency to over-estimate this flux here. Exact correspondence with observations is not expected given the high degree of inter-annual variability of the carbon budget terms. For the European Shelf as a whole, inputs of carbon from rivers and the uptake of CO_2 from the atmosphere are balanced by horizontal transport off shelf, with a net transport of $6 \pm 1 \times 10^{12} \text{ mol C yr}^{-1}$. Both the large-scale circulation and the biological carbon pump contribute significantly to the export of carbon from the shelf. More than half of the off-shelf carbon transport occurs below 180 m depth – in the bottom 20 m of the water column across the 200 m isobath on the shelf and in the deep waters of the Norwegian Trench – and hence potentially may be exported below the permanent pycnocline to the deep waters of the North Atlantic. The near-bed off-shelf transport of carbon supports the carbon pump hypothesis for the northwest European continental shelf.

[49] **Acknowledgments.** This work was funded by the NERC National Centre for Earth Observation, and the National Capability in Modeling at the National Oceanography Centre and the Plymouth Marine Laboratory. We thank H. Thomas (Dalhousie University, Canada) and A. V. Borges (Université de Liège, Belgium) for supplying DIC observations in the North Sea, J. Remedios and R. Leigh (University of Leicester, UK) for atmospheric CO_2 data appropriate for the northeast Atlantic and T. Smyth (Plymouth Marine Laboratory, UK) for IOP estimates from SeaWiFS.

References

Allen, J. I., J. T. Holt, J. C. Blackford, and R. Proctor (2007), Error quantification of a high resolution coupled hydrodynamic-ecosystem coastal-

- ocean model: Part 2. Chlorophyll-a, nutrients and SPM, *J. Mar. Syst.*, 68(3–4), 381–404, doi:10.1016/j.jmarsys.2007.01.005.
- Artoli, Y., J. C. Blackford, M. Butenschön, J. T. Holt, S. L. Wakelin, H. Thomas, A. V. Borges, and I. Allen (2012), The carbonate system in the North Sea: Sensitivity and model validation, *J. Mar. Syst.*, in press.
- Bellerby, R. G. J., A. Olsen, T. Furevik, and L. A. Anderson (2005), Response of the surface ocean CO_2 system in the Nordic seas and northern North Atlantic to climate change, in *The Nordic Seas: An Integrated Perspective Oceanography, Climatology, Biogeochemistry, and Modeling*, *Geophys. Monogr. Ser.*, vol. 158, edited by H. Drange *et al.*, pp. 189–197, AGU, Washington, D. C., doi:10.1029/158GM13.
- Blackford, J. C., and F. J. Gilbert (2007), pH variability and CO_2 induced acidification in the North Sea, *J. Mar. Syst.*, 64(1–4), 229–241, doi:10.1016/j.jmarsys.2006.03.016.
- Blackford, J. C., J. I. Allen, and F. J. Gilbert (2004), Ecosystem dynamics at six contrasting sites: A generic model study, *J. Mar. Syst.*, 52(1–4), 191–215, doi:10.1016/j.jmarsys.2004.02.004.
- Borges, A. V. (2005), Do we have enough pieces of the jigsaw to integrate CO_2 fluxes in the coastal ocean?, *Estuaries*, 28(1), 3–27, doi:10.1007/BF02732750.
- Borges, A. V., and M. Frankignoulle (2002), Distribution of surface carbon dioxide and air-sea exchange in the upwelling system off the Galician coast, *Global Biogeochem. Cycles*, 16(2), 1020, doi:10.1029/2000GB001385.
- Borges, A. V., and M. Frankignoulle (2003), Distribution of carbon dioxide and air-sea exchange in the English Channel and adjacent areas, *J. Geophys. Res.*, 108(C5), 3140, doi:10.1029/2000JC000571.
- Borges, A. V., L.-S. Schiettecatte, G. Abril, B. Delille, and F. Gazeau (2006), Carbon dioxide in European coastal waters, *Estuarine Coastal Shelf Sci.*, 70, 375–387, doi:10.1016/j.ecss.2006.05.046.
- Bozec, Y., H. Thomas, K. Elkalay, and H. J. W. de Baar (2005), The continental shelf pump for CO_2 in the North Sea—Evidence from summer observation, *Mar. Chem.*, 93, 131–147, doi:10.1016/j.marchem.2004.07.006.
- Chen, C.-T. A., and A. V. Borges (2009), Reconciling opposing views on carbon cycling in the coastal ocean: Continental shelves as sinks and near-shore ecosystems as sources of atmospheric CO_2 , *Deep Sea Res., Part II*, 56, 578–590, doi:10.1016/j.dsr2.2009.01.001.
- Dickson, A. G., and F. J. Millero (1987), A comparison of the equilibrium constants for the dissociation of carbonic acid in seawater media, *Deep Sea Res.*, 34, 1733–1743, doi:10.1016/0198-0149(87)90021-5.
- Fairall, C. W., E. F. Bradley, J. E. Hare, A. A. Grachev, and J. B. Edson (2003), Bulk parameterization of air-sea fluxes: Updates and verification for the COARE algorithm, *J. Clim.*, 16, 571–591, doi:10.1175/1520-0442(2003)016<0571:BPOASF>2.0.CO;2.
- Fennel, K. (2010), The role of continental shelves in nitrogen and carbon cycling: Northwestern North Atlantic case study, *Ocean Sci.*, 6, 539–548, doi:10.5194/os-6-539-2010.
- Fennel, K., and J. Wilkin (2009), Quantifying biological carbon export for the northwest North Atlantic continental shelves, *Geophys. Res. Lett.*, 36, L18605, doi:10.1029/2009GL039818.
- Fennel, K., J. Wilkin, M. Previdi, and R. Najjar (2008), Denitrification effects on air-sea CO_2 flux in the coastal ocean: Simulations for the northwest North Atlantic, *Geophys. Res. Lett.*, 35, L24608, doi:10.1029/2008GL036147.
- Flather, R. A. (1981), Results from a model of the northeast Atlantic relating to the Norwegian Coastal Current, in *The Norwegian Coastal Current*, vol. 2, edited by R. Saetre and M. Mork, pp. 427–458, Bergen Univ., Bergen, Norway.
- Frankignoulle, M., and A. V. Borges (2001), European continental shelf as a significant sink for atmospheric carbon dioxide, *Global Biogeochem. Cycles*, 15(3), 569–576, doi:10.1029/2000GB001307.
- Frankignoulle, M., G. Abril, A. Borges, I. Bourge, C. Canon, B. Delille, E. Libert, and J.-M. Théate (1998), Carbon dioxide emission from European estuaries, *Science*, 282, 434–436, doi:10.1126/science.282.5388.434.
- Garcia, H. E., R. A. Locarnini, T. P. Boyer, and J. I. Antonov (2006), *World Ocean Atlas 2005*, vol. 4, *Nutrients (Phosphate, Nitrate, Silicate)*, NOAA Atlas NESDIS, vol. 64, edited by S. Levitus, 396 pp., U.S. Gov. Print. Off., Washington, D. C.
- Gypens, N., C. Lancelot, and A. V. Borges (2004), Carbon dynamics and CO_2 air-sea exchanges in the eutrophied coastal waters of the Southern Bight of the North Sea: A modelling study, *Biogeosciences*, 1, 147–157, doi:10.5194/bg-1-147-2004.
- Gypens, N., A. V. Borges, and C. Lancelot (2009), Effect of eutrophication on air-sea CO_2 fluxes in the coastal Southern North Sea: A model study of the past 50 years, *Global Change Biol.*, 15(4), 1040–1056, doi:10.1111/j.1365-2486.2008.01773.x.
- Holt, J. T., and I. D. James (1999), A simulation of the Southern North Sea in comparison with measurements from the North Sea Project.

- Part 2: Suspended particulate matter, *Cont. Shelf Res.*, 19, 1617–1642, doi:10.1016/S0278-4343(99)00032-1.
- Holt, J. T., and I. D. James (2001), An s-coordinate density evolving model of the north west European continental shelf: 1 Model description and density structure, *J. Geophys. Res.*, 106(C7), 14,015–14,034, doi:10.1029/2000JC000304.
- Holt, J. T., J. I. Allen, R. Proctor, and F. Gilbert (2005), Error quantification of a high resolution coupled hydrodynamic-ecosystem coastal-ocean model: Part I Model overview and assessment of the hydrodynamics, *J. Mar. Syst.*, 57, 167–188, doi:10.1016/j.jmarsys.2005.04.008.
- Holt, J., S. Wakelin, and J. Huthnance (2009), Down-welling circulation of the northwest European continental shelf: A driving mechanism for the continental shelf pump, *Geophys. Res. Lett.*, 36, L14602, doi:10.1029/2009GL038997.
- Holt, J., M. Butenschön, S. L. Wakelin, Y. Artioli, and J. I. Allen (2012), Oceanic controls on the primary production of the northwest European continental shelf: model experiments under recent past conditions and a potential future scenario, *Biogeosciences*, 9, 97–117, doi:10.5194/bg-9-97-2012.
- Huthnance, J. M. (1995), Circulation, exchange and water masses at the ocean margin: the role of physical processes at the shelf edge, *Prog. Oceanogr.*, 35(4), 353–431.
- Ingri, N., W. Kakolowicz, L. G. Sillén, and B. Warnqvist (1967), High-speed computers as a supplement to graphical methods—V: Haltafall, a general program for calculating the composition of equilibrium mixtures, *Talanta*, 14(11), 1261–1286, doi:10.1016/0039-9140(67)80203-0.
- Kim, H.-C., and K. Lee (2009), Significant contribution of dissolved organic matter to seawater alkalinity, *Geophys. Res. Lett.*, 36, L20603, doi:10.1029/2009GL040271.
- Kühn, W., J. Pätsch, H. Thomas, A. V. Borges, L.-S. Schiettecatte, Y. Bozec, and A. E. F. Prowe (2010), Nitrogen and carbon cycling in the North Sea and exchange with the North Atlantic—A model study, part II: Carbon budget and fluxes, *Cont. Shelf Res.*, 30(16), 1701–1716, doi:10.1016/j.csr.2010.07.001.
- Lenhart, H. J., J. Pätsch, W. Kühn, A. Moll, and T. Pohlmann (2004), Investigation on the trophic state of the North Sea for three years (1994–1996) simulated with the ecosystem model ERSEM—The role of a sharp NAOI decline, *Biogeosci. Discuss.*, 1, 725–754, doi:10.5194/bgd-1-725-2004.
- Le Quéré, C., et al. (2009), Trends in the sources and sinks of carbon dioxide, *Nat. Geosci.*, 2, 831–836, doi:10.1038/ngeo689.
- Lewis, K., J. I. Allen, A. J. Richardson, and J. T. Holt (2006), Error quantification of a high resolution coupled hydrodynamic-ecosystem coastal-ocean model: Part 3. Validation with continuous plankton recorder data, *J. Mar. Syst.*, 63(3–4), 209–224, doi:10.1016/j.jmarsys.2006.08.001.
- Mehrbach, C., C. H. Culbertson, J. E. Hawley, and M. Pytkowicz (1973), Measurement of the apparent dissociation constant of carbonic acid in seawater at atmospheric pressure, *Limnol. Oceanogr.*, 18, 897–907, doi:10.4319/lo.1973.18.6.0897.
- Nightingale, P. D., G. Malin, C. S. Law, A. J. Watson, P. S. Liss, M. I. Liddicoat, J. Boutin, and R. C. Upstill-Goddard (2000), In situ evaluation of air-sea gas exchange parameterizations using novel conservative and volatile tracers, *Global Biogeochem. Cycles*, 14(1), 373–387, doi:10.1029/1999GB000091.
- Pätsch, J., and H. J. Lenhart (2004), Daily loads of nutrients, total alkalinity, dissolved inorganic carbon and dissolved organic carbon of the European continental rivers for the years 1977–2002, *Ber. aus dem Zent. für Meeres-und Klimaforsch., Reihe B, Ozeanogr.*, 48, 159 pp., Inst. für Meereskunde, Hamburg, Germany.
- Pope, R. M., and E. S. Fry (1997), Absorption spectrum (380–700 nm) of pure water. II. Integrating cavity measurements, *Appl. Opt.*, 36, 8710–8723, doi:10.1364/AO.36.008710.
- Prowe, A. E. F., H. Thomas, J. Pätsch, W. Kühn, Y. Bozec, L.-S. Schiettecatte, A. V. Borges, and H. J. W. de Baar (2009), Mechanisms controlling the air-sea CO₂ flux in the North Sea, *Cont. Shelf Res.*, 29(15), 1801–1808, doi:10.1016/j.csr.2009.06.003.
- Raymond, P. A., and J. J. Cole (2003), Increase in the export of alkalinity from North America's largest river, *Science*, 301, 88–91, doi:10.1126/science.1083788.
- Rowe, G. T., and J. W. Deming (1985), The role of bacteria in the turnover of organic carbon in deep-sea sediments, *J. Mar. Res.*, 43, 925–950, doi:10.1357/002224085788453877.
- Sabine, C. L., et al. (2004), The oceanic sink for anthropogenic CO₂, *Science*, 305(5682), 367–371, doi:10.1126/science.1097403.
- Schiettecatte, L.-S., F. Gazeau, C. Van der Zee, N. Brion, and A. V. Borges (2006), Time series of the partial pressure of carbon dioxide (2001–2004) and preliminary inorganic carbon budget in the Scheldt plume (Belgian coast waters), *Geochem. Geophys. Geosyst.*, 7, Q06009, doi:10.1029/2005GC001161.
- Schiettecatte, L.-S., H. Thomas, Y. Bozec, and A. V. Borges (2007), High temporal coverage of carbon dioxide measurements in the Southern Bight of the North Sea, *Mar. Chem.*, 106, 161–173, doi:10.1016/j.marchem.2007.01.001.
- Schuster, U., and A. J. Watson (2007), A variable and decreasing sink for atmospheric CO₂ in the North Atlantic, *J. Geophys. Res.*, 112, C11006, doi:10.1029/2006JC003941.
- Schuster, U., A. J. Watson, N. R. Bates, A. Corbiere, M. Gonzalez-Davila, N. Metzl, D. Pierrot, and M. Santana-Casiano (2009), Trends in North Atlantic sea-surface fCO₂ from 1990 to 2006, *Deep Sea Res., Part II*, 56, 620–629, doi:10.1016/j.dsr2.2008.12.011.
- Smith, G., and K. Haines (2009), Evaluation of the S(T) assimilation method with the Argo dataset, *Q. J. R. Meteorol. Soc.*, 135, 739–756, doi:10.1002/qj.395.
- Smith, R. S., and J. Marotzke (2008), Factors influencing anthropogenic carbon dioxide uptake in the North Atlantic in models of the ocean carbon cycle, *Clim. Dyn.*, 31, 599–613, doi:10.1007/s00382-008-0365-y.
- Smyth, T. J., G. F. Moore, T. Hirata, and J. Aiken (2006), Semianalytical model for the derivation of ocean color inherent optical properties: Description, implementation, and performance assessment, *Appl. Opt.*, 45, 8116–8131, doi:10.1364/AO.45.008116.
- Song, Y., and D. Haidvogel (1994), A semi-implicit ocean circulation model using a generalized topography-following coordinate system, *J. Comput. Phys.*, 115, 228–244, doi:10.1006/jcph.1994.1189.
- Souza, A. J., J. H. Simpson, M. Harikrishnan, and J. Malarkey (2001), Flow structure and seasonality in the Hebridean slope current, *Oceanol. Acta*, 24, suppl. 1, 63–76, doi:10.1016/S0399-1784(00)01103-8.
- Suykens, K., B. Delille, L. Chou, C. De Bodt, J. Harlay, and A. V. Borges (2010), Dissolved inorganic carbon dynamics and air-sea carbon dioxide fluxes during coccolithophore blooms in the Northwest European continental margin (northern Bay of Biscay), *Global Biogeochem. Cycles*, 24, GB3022, doi:10.1029/2009GB003730.
- Takahashi, T., T. T. Takahashi, and S. C. Sutherland (1995), An assessment of the role of the North Atlantic as a CO₂ sink, *Philos. Trans. R. Soc. London, Ser. B*, 348, 143–152, doi:10.1098/rstb.1995.0056.
- Takahashi, T., et al. (2002), Global sea-air CO₂ flux based on climatological surface ocean pCO₂, and seasonal biological and temperature effects, *Deep Sea Res., Part II*, 49(9–10), 1601–1622, doi:10.1016/S0967-0645(02)00003-6.
- Takahashi, T., et al. (2009), Climatological mean and decadal change in surface ocean pCO₂, and net sea-air CO₂ flux over the global oceans, *Deep Sea Res., Part II*, 56(8–10), 554–577, doi:10.1016/j.dsr2.2008.12.009.
- Thomas, H. (2002), The continental shelf pump hypothesis: A pilot study in the North Sea (CANOBA), shipboard report of the RV *Pelagia* cruises 64PE184, 64PE187, 64PE190 and 64PE195, 63 pp., R. Neth. Inst. of Sea Res., Texel, Netherlands.
- Thomas, H., J. Pempkowiak, F. Wulff, and K. Nagel (2003), Autotrophy, nitrogen accumulation and nitrogen limitation in the Baltic Sea: A paradox or a buffer for eutrophication?, *Geophys. Res. Lett.*, 30(21), 2130, doi:10.1029/2003GL017937.
- Thomas, H., Y. Bozec, K. Elkalay, and H. J. W. de Baar (2004), Enhanced open ocean storage of CO₂ from shelf sea pumping, *Science*, 304, 1005–1008, doi:10.1126/science.1095491.
- Thomas, H., Y. Bozec, H. J. W. de Baar, K. Elkalay, M. Frankignoulle, L.-S. Schiettecatte, G. Kattner, and A. V. Borges (2005a), The carbon budget of the North Sea, *Biogeosciences*, 2, 87–96, doi:10.5194/bg-2-87-2005.
- Thomas, H., Y. Bozec, K. Elkalay, H. J. W. de Baar, A. V. Borges, and L.-S. Schiettecatte (2005b), Controls of the surface water partial pressure of CO₂ in the North Sea, *Biogeosciences*, 2, 323–334, doi:10.5194/bg-2-323-2005.
- Thomas, H., L.-S. Schiettecatte, K. Suykens, Y. J. M. Koné, E. H. Shadwick, A. E. F. Prowe, Y. Bozec, H. J. W. de Baar, and A. V. Borges (2009), Enhanced ocean carbon storage from anaerobic alkalinity generation in coastal sediments, *Biogeosciences*, 6, 267–274, doi:10.5194/bg-6-267-2009.
- Tsunogai, S., S. Watanabe, and T. Sato (1999), Is there a “continental shelf pump” for the absorption of atmospheric CO₂?, *Tellus, Ser. B*, 51, 701–712, doi:10.1034/j.1600-0889.1999.t01-2-00010.x.
- Wakelin, S. L., J. T. Holt, and R. Proctor (2009), The influence of initial conditions and open boundary conditions on shelf circulation in a 3D ocean-shelf model of the north east Atlantic, *Ocean Dyn.*, 59, 67–81, doi:10.1007/s10236-008-0164-3.
- Yool, A., and M. J. R. Fasham (2001), An examination of the “continental shelf pump” in an open ocean general circulation model, *Global Biogeochem. Cycles*, 15, 831–844, doi:10.1029/2000GB001359.
- Young, E. F., and J. T. Holt (2007), Prediction and analysis of long-term variability of temperature and salinity in the Irish Sea, *J. Geophys. Res.*, 112, C01008, doi:10.1029/2005JC003386.